IEEE Access
Multidisciplinary | Rapid Review | Open Access Journal

Received February 9, 2021, accepted February 23, 2021, date of publication March 1, 2021, date of current version March 11, 2021.

Digital Object Identifier 10.1109/ACCESS.2021.3062895

Secrecy Energy Efficiency Maximization for UAV Swarm Assisted Multi-Hop Relay System: Joint Trajectory Design and Power Control

JIANSONG MIAO, HAIRUI LI, ZIYUAN ZHENG, AND CHU WANG

Beijing Laboratory of Advanced Information Networks, Beijing University of Posts and Telecommunications, Beijing 100876, China

Corresponding author: Hairui Li (lhr@bupt.edu.cn)

This work was supported by Natural Science Foundation of Beijing Municipality under Grant L192034.

ABSTRACT Unmanned aerial vehicle (UAV) relay can effectively improve the coverage and performance of land communications, which makes it prospective to be deployed in various applications. However, there exist some practical challenges we have to face in UAV-enabled communication system designing, such as secrecy and wiretapping threats due to the air-to-ground line-of-sight communication link, and energy consumption issues because of the limitation in energy-constraint. To deal with these two key issues, we develop a novel UAV swarm assisted multi-hop mobile relay system which can be applied in special scenarios with severe blockage or long distance to enhance communication performance. An effective cooperative transmission scheme is proposed to address the security issues in a physical layer security perspective, where several UAVs serve as multi-hop relays forwarding information between ground users and the other UAVs are employed as friendly jammers confusing the ground eavesdroppers. The minimum secrecy energy efficiency (MSEE), namely the minimum achievable secrecy rate per energy consumption unit over legitimate links, is designed as the performance indicator to quantify the secure and energy-efficient transmission. Subject to information-causality, transmit power, and mobility constraints, the UAV swarm assisted MSEE maximization transmission scheme is formulated into a complicated non-convex problem. To solve the non-convex fractional optimization problem, we decouple the original problem into sub-problems and further propose an efficient algorithm by applying the block coordinate descent method, successive convex approximation (SCA) techniques, and Dinkelbach method. Numerical results demonstrate that the proposed scheme achieves considerable performance enhancement on MSEE compared with benchmark schemes.

INDEX TERMS UAV swarm, multi-hop relay, energy efficiency, physical layer security.

I. INTRODUCTION

Recently, unmanned aerial vehicles (UAVs) communication has attracted more and more attention and become a new hot spot in wireless communication fields, due to its unique advantages, such as high flexibility, on-demand deployment, quick networking, line-of-sight (LOS) information transmission, etc [1]. These valuable characteristics make the UAV-enabled communication system have a great prospect in various application requirements [2], e.g., disaster recovery, data collecting in Internet of Things (IoT), aerial imaging, and industrial monitoring. Moreover, with the evolution of the 5G/6G terrestrial networks, UAV-enabled wireless system, as non-terrestrial network for necessary compensation, will play an essential role in providing ubiquitous access for some special scenarios where terrestrial infrastructures are not available for users [3]. In the UAV-enabled communication system, UAVs can not only be employed as mobile base stations to serve a group of ground users for better wireless coverage [4], [5] but also act as mobile relays for information forwarding between ground users where direct links are not available for them [6], [7]. The authors in [4] propose a polynomial-time algorithm for optimal UAV placement to minimize the number of UAVs required for covering all the ground terminals. The study in [5] is to maximize system throughput, and an iterative algorithm is proposed based on joint optimization of UAV's trajectory and transmit power. Reference [6] maximizes the throughput of a UAV-enabled relay system by jointly optimizing the UAV's trajectory and transmit power, and the works in [7] examine the mobile

The associate editor coordinating the review of this manuscript and approving it for publication was Cong Pu.

TABLE 1. Summary to references [11]–[16].

Reference	Density, Type and Mobility of UAV Transmitter	Type and Location of Ground Users	Density and Location of Eavesdroppers	Deployment Environment	Objective	Optimization Methods
Zhou et al.[11]	Single UAV/Base Station/Mobile	Multiple GUs/Exactly	Multiple GEs/Exactly	Not Special	Maximizing the Minimum Average Secrecy Rate	BCD and SCA
Li et al.[12]	Single UAV/Base Station/Mobile	Single GU/Exactly	Multiple GEs/Inexactly	Not Special	Maximizing the Worst-case Secrecy Rate	BCD and SCA
Li et al.[13]	Two UAVs/Base Station/Mobile	Multiple GUs/Exactly	Multiple GEs/Exactly	Special (with NFZ)	Maximizing the Minimum Average Secrecy Rate	BCD and SCA
Tang et al.[14]	N/A	Two GUs/Exactly	Multiple UEs/BPP	Suburban	Analyzing the System Secure Connection Probability	Monte Carlo Trial
Ma et al.[15]	Multiple UAVs/ Relay/Fixed	Two GUs/Exactly	Multiple GEs/PPP	Not Special	Analyzing the System Secrecy Outage Probability	Monte Carlo Trial
Zhang et al.[16]	Single UAV/Base Station/Mobile	Multiple GUs/Exactly	Multiple GEs/Exactly	Urban	Maximizing the System Secrecy Capacity	CAA-MADDPG

GU = Ground User, GE= Ground Eavesdropper, UE = UAV Eavesdropper; NFZ = No-Fly-Zone, BCD = Block Coordinate Descent.

relay system reliability performance which is represented by outage probability.

A. RELATED WORK AND MOTIVATION

Although great progress has been made in the UAV-enabled wireless system from different requirements and perspectives, including better coverage, throughput maximization, communication reliability, etc, there still exist many issues waiting to be solved. For example, the physical layer security problem including passive eavesdropping and active eavesdropping is tricky due to the high probability of LOS air-to-ground channel. Specifically, on one hand, the information transmission is insecure and likely to be wiretapped by the undesired receivers, which leads to a risk of information leakage. On the other hand, legitimate links are vulnerable to malicious jamming attacks. By optimizing the UAV's trajectory, [8] maximizes the average secrecy rates of both the UAV-to-ground and ground-to-UAV transmissions. And the block coordinate descent method and successive convex approximation techniques are applied to handle the non-convex problem. A millimeter-Wave simultaneous wireless information and power transfer (SWIPT) UAV network based on nonorthogonal multiple access (NOMA) is studied in [9], the antenna selection of directional modulation is optimized via applying adaptive genetic simulated annealing algorithm to improve the system security performance. Reference [10] investigates a two-tier UAV network consisting of multiple UAV transmitters and receivers, and proposes a matching algorithm and overlapping coalition formation algorithm to provide secure communication for multiple legitimate links.

For further improvement on the system secrecy performance, [11]–[16] introduce a friendly jammer UAV to confuse the eavesdropping link. However, when the jammer UAV flies closer to legitimate users, the confidential information transmission is vulnerable to be destroyed. Therefore, the design on the jammer UAV trajectory and power is required in UAV-assisted wireless communication. Especially, [11] shows that a UAV as a jammer can improve the average secrecy rate over all receivers by jointly optimizing trajectory and transmit power in a UAV-enabled base station system. Reference [12] explores a similar system where the position information is unknown, aiming at maximizing the worst-case secrecy rate of the system. To achieve a higher rate in secure communications, multi-purpose UAV base stations are adopted in [13], where the sub-carrier allocation and UAV trajectory are jointly optimized. The works [11]–[13] optimize the objective in a similar method by decoupling the original problem into several sub-problems and solving them in an iterative manner. However, [14] considers a novel situation with multiple UAV eavesdroppers (UEs) of inexact position, and analyzes the system secure connection probability by Monte Carlo trial. An opportunistic relay selection scheme is investigated in a millimeter wave communication system where exists multiple randomly distributed ground eavesdroppers [15]. Reference [16] designs a UAV trajectory 3D space optimization scheme and proposes a continuous action attention multi-agent deep deterministic policy gradient (CAA-MADDPG) method to maximize the system secure capacity. For reader convenience, the crucial parameters and optimization methods of reviewed works [11]–[16] are provided in Table 1.

Apart from security issues, the UAV's working time is restricted by the limited onboard energy, which poses a bottleneck for system performance. Therefore, much research has been conducted on UAV energy consumption. Reference [17] derives a propulsion energy consumption model of fixed-wing UAV based on the UAV's flying speed, direction, and acceleration and optimizes the UAV trajectory by jointly considering the communication throughput and energy consumption, while the works in [18] minimize the rotary-wing UAV energy consumption, including both propulsion energy consumption and communication-related consumption. The study in [19] maximizes the system secrecy energy efficiency by jointly optimizing the UAV trajectory, transmit

power, and user scheduling via applying the block coordinate descent method and Dinkelbach method in combination with successive convex approximation techniques. However, the innovation works in [19] are only limited to the UAV-enabled base station system, while a multi-hop UAV relay system is investigated in this article.

There exists much research to explore the secrecy rate maximization problem in UAV-enabled mobile relay system with a cooperative jammer UAV [20]. However, the single UAV relay model is not applicable in the scenario where the distance between the source and destination is too long. Reference [21] shows that multi-hop UAV relay can effectively increase the communication distance and resolve the link blockage problem caused by obstacles or terrains, but it does not consider security issues. Therefore, a UAV-assisted multi-hop relay system with cooperative jammers needs to be studied to hence the secrecy performance.

In this article, our work sets out to propose a novel UAV swarm cooperative scheme in the presence of multiple eavesdroppers to explore the secrecy energy efficiency (SEE) performance in a multi-hop mobile relay system. In this swarm, UAVs are allocated into two groups according to their different tasks: the relay UAVs (RUAVs) for information forwarding from source to destination, and the jammer UAVs (JUAVs) acting as friendly jammers to enhance the legitimate link secrecy performance by introducing active interference to eavesdroppers. To enhance the spectrum efficiency, we assume that the JUAVs share the same bandwidth with all RUAVs, so the JUAVs' transmit power should be designed to mitigate the co-channel interference. In a decode-and-forward (DF) multi-hop relay system, the end-to-end throughput is limited by the weakest link [21], [22]. Therefore, we maximize the average minimum secrecy energy efficiency (MSEE) via jointly optimizing the UAV trajectory and transmit power with an efficient iterative algorithm. Until now no existing studies have been reported in current literatures on the minimum secrecy energy efficiency maximization for UAV swarm assisted multi-hop mobile relay system. Therefore, we carry out this research work and try to push forward the field for a new step.

B. CONTRIBUTION

The main contributions of our work are as follows:

- This article presents a novel UAV swarm assisted multi-hop relay model to improve the secrecy and energy efficiency performance for deployment in a severe blockage and long distance scenario. In this model, the RUAVs are deployed as multi-hop relays for cooperative information forwarding, while the JUAVs acting as friendly jammers confuse the eavesdroppers to ensure confidential information transmission. Then, We formulate a minimum secrecy energy efficiency MSEE) maximization problem by jointly optimizing the swarm's flight trajectory and transmit power over all time slots, subject to the constraints of UAV mobility, transmit power, and information-causality. Note that the formulated problem is quite complex and hard to deal with, because of the non-convexity of objective and constraints, fractional form, and tightly coupled optimizing variables.
- To handle the non-convex fractional optimization problem, an efficient iterative algorithm is proposed. First, we decouple the original optimization problem into four sub-problems to solve them iteratively by applying block coordinate descent. Next, the successive convex approximation technique is used to transform non-convex objective functions or constraints into convex forms. However, the trajectory optimization sub-problems with fractional object functions are still challenging to handle, and therefore, we apply the Dinkelbach method to solve it. The solution can be eventually obtained in an iterative manner until the MSEE increment is below a threshold, and the convergence of the proposed iterative algorithm is demonstrated finally.
- Sufficient simulations are conducted to evaluate the effectiveness of our proposed scheme. We observe the features of trajectory, velocity, and transmit power at each time slot, and explore the diversity of trajectory and MSEE in different schemes. The results show that the proposed scheme achieves significant improvements on secrecy energy efficiency performance compared with another three benchmarks.

The rest of this article is organized as follows. In Section II, we introduce the UAV swarm assisted multi-hop mobile relay system model and formulate the SEE optimization problem. Section III presents an efficient iterative scheme to solve the formulated complex problem by using the block coordinate descent method, Dinkelbach method, and SCA techniques, and the overall algorithm is demonstrated at the end of this section. In Section IV, the simulation results and discussion are provided to illustrate the superiority of our scheme. Finally, we conclude this article in Section V.

II. SYSTEM MODEL AND PROBLEM FORMULATION

A. SYSTEM MODEL

As shown in Figure 1, we consider a UAV swarm-assisted multi-hop mobile relay system where $M > 1$ RUAVs are employed to forward confidential information between a ground source user (S) and a legitimate ground destination user (D). To improve secrecy performance in the system, we introduce $L \geq 1$ JUAVs as friendly jammers to combat against $K \geq 1$ passive eavesdroppers. The RUAV, JUAV and eavesdropper sets are denoted as $\mathcal{R}$, $\mathcal{J}$ and $\mathcal{E}$, respectively, where $|\mathcal{R}| = M$, $|\mathcal{J}| = L$, and $|\mathcal{E}| = K$. We assume that the users provide their locations for UAV swarm actively, and all the UAVs fly at a fixed altitude of H, which can be considered as the minimum altitude to avoid collision by infrastructure obstacles. Besides, the locations of eavesdroppers can be detected from the local oscillator power unintentionally leaking from the radio frequency front end [16], [23]. Therefore,

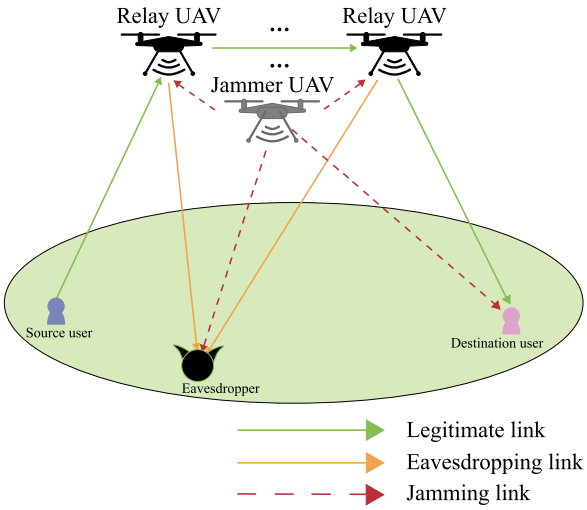

FIGURE 1. An illustration of UAV swarm assisted multi-hop relay system.

we assume the UAV swarm can exactly know the locations of S, D, $\mathcal{E}$ and exchange information instantly [11], [16]. The UAVs' collisions are not considered here, which can be readily extended by introducing the minimum security distance constraints.

Without loss of generality, a three-dimensional Cartesian coordinate system is adopted in this article. The horizontal coordinate of ground nodes can be denoted by $\mathbf{w}_i = [x_i, y_i]^T$ in meter (m), $i \in \{\mathrm{S}, \mathrm{D}, \mathcal{E}\}$. The UAV flight period T is discretized into N equal-length time slots, i.e., $T = N\delta$, where δ denotes the elemental slot length. And we set that the UAV j flies with the pre-determined initial location $\mathbf{q}_{j_0}$ and final location $\mathbf{q}_{j_F}$, where $j \in \{\mathcal{R}, \mathcal{J}\}$. To simplify the optimization problem, UAV trajectory over T can be constructed by using line-segment to connect the optimized N discrete locations $\mathbf{q}_j[n] = \left[x_j[n], y_j[n]\right]^T$, where $j \in \{\mathcal{R}, \mathcal{J}\}, n \in \mathcal{N} = \{1, \ldots, N\}$. The locations of each UAV in adjacent time slots satisfy the following mobility constraints:

$$\left\|\mathbf{q}_j[n+1] - \mathbf{q}_j[n]\right\|^2 \le (V_{max}\delta)^2, j \in \{\mathcal{R}, \mathcal{J}\}, \quad (1)$$

$$n = 1, \ldots, N-1,$$

$$\mathbf{q}_j[1] = \mathbf{q}_{j_0}, \mathbf{q}_j[N] = \mathbf{q}_{j_F}, j \in \{\mathcal{R}, \mathcal{J}\}, \quad (2)$$

where $V_{max}\delta$ is the maximum horizontal distance that UAV can fly within one time slot under its maximum flight speed V_{max} in m/s.

The communication links in the UAV assisted multi-hop relay system are classified and handled as follows: 1) Legitimate link: S-to-R, R-to-R, and R-to-D, where confidential information can be transmitted; 2) Eavesdropping link: R-to-E, where the ground eavesdropper E_k wiretaps the RUAVs; 3) Jamming link: J-to-E, J-to-R, and J-to-D, where the signals transmitted by the JUAVs are regarded as noise for other terminals, i.e., R, D. According to the node position of each link [2], the S-to-R, J-to-D/E and R-to-D/E link can be regarded as air-to-ground (A2G) channel, and R-to-R and J-to-R are air-to-air (A2A) channel links. In general, the A2G channel includes both line-of-sight (LOS) and non-line-of-sight (NLOS) paths, due to the ground reflection, building scattering, and so on. It is still a challenge to model the complex effects, and the probabilistic LOS model is used in [24], [25]. In contrast, the A2A channel with few obstacles has higher probability of LOS link, but larger Doppler effect caused by higher relative velocity. To draw most essential insights and for ease of exposition, we assume that both A2G and A2A communications are dominated by LOS links [26], and the Doppler effect caused by UAV's mobility is also assumed to be perfectly compensated. Therefore, we adopt free-space path loss model as used in [4], [8], [27] to model each link. The power gain of the A2G channel at time slot n can be written as

$$h_{j,i}[n] = \rho_0 d_{j,i}^{-2}[n] = \frac{\rho_0}{\left\|\mathbf{q}_j[n] - \mathbf{w}_i[n]\right\|^2 + H^2}, n \in \mathcal{N}, \quad (3)$$

where ρ_0 denotes the channel power at reference distance $d_0 = 1m$, and $j \in \{\mathcal{R}, \mathcal{J}\}, i \in \{\mathrm{S}, \mathrm{D}, \mathcal{E}\}$, so $d_{j,i}$ and $h_{j,i}$ denote the distance and the channel gain from RUAV R_m or JUAV J_l to the ground terminal S, D or eavesdropper E_k, respectively.

Similarly, the power gain of the A2A channel at time slot n can be written as

$$h_{j,j^*}[n] = \rho_0 d_{j,j^*}^{-2}[n] = \frac{\rho_0}{\left\|\mathbf{q}_j[n] - \mathbf{q}_{j^*}[n]\right\|^2}, \quad n \in \mathcal{N}, \quad (4)$$

where $j, j^* \in \{\mathcal{R}, \mathcal{J}\}$, so d_{j,j^*} and h_{j,j^*} denote the distance and the channel gain from RUAV R_m to another RUAV R_{m^*} or JUAV J_l respectively.

Since we only consider the energy consumption of UAV swarm, the transmit power of S can be fixed by P_S. The transmit power of RUAV m and JUAV l is denoted as P_{R_m} and P_{J_l}, respectively, subject to maximum transmit power constraints as follows

$$0 \le P_{R_m}[n] \le P_{R_{max}}, n \in \mathcal{N}, m \in \mathcal{M}, \quad (5)$$

$$0 \le P_{J_l}[n] \le P_{J_{max}}, n \in \mathcal{N}, l \in \mathcal{L}. \quad (6)$$

The maximum transmit power constraint of UAV at each time slot is related to the limitation of the real-time transmit power of the device.

By assuming that all the UAVs are equipped with a data buffer of sufficiently large size and operate in a frequency division duplexing (FDD) mode with equal bandwidth allocated for each legitimate link. The achievable rates of S-to-R_1 link and R_M-to-D link in bit/second/Hz (bps/Hz) at slot n can be expressed as

$$R_{SR_1}[n] = \log_2\left(1 + \frac{P_S \hat{h}_{SR_1}[n]}{\sum_{l=1}^{L} P_{J_l}[n]\hat{h}_{J_l R_1}[n] + 1}\right), \quad (7)$$

$$R_{R_M D}[n] = \log_2\left(1 + \frac{P_{R_M}[n]\hat{h}_{R_M D}[n]}{\sum_{l=1}^{L} P_{J_l}[n]\hat{h}_{J_l D}[n] + 1}\right), \quad (8)$$

where $\hat{h}_{jj^*}[n] = \frac{\gamma_0}{\|\mathbf{q}_j[n]-\mathbf{q}_{j^*}[n]\|^2}, j, j^* \in \{\mathcal{R}, \mathcal{J}\}, j \neq j^*, n \in \mathcal{N}$, $\hat{h}_{ji}[n] = \frac{\gamma_0}{\|\mathbf{q}_j[n]-\mathbf{w}_i[n]\|^2+H^2}, j \in \{\mathcal{R}, \mathcal{J}\}, i \in \{\mathrm{S}, \mathrm{D}, \mathcal{E}\}, n \in \mathcal{N}, \gamma_0 = \frac{\rho_0}{\sigma^2}$, and σ^2 denotes the noise power.

Similarly, the achievable rate of R_m-to-R_{m+1} link in bps/Hz at time slot n can be expressed as

$$R_{R_mR_{m+1}}[n] = \log_2\left(1 + \frac{P_{R_m}[n]\hat{h}_{R_mR_{m+1}}[n]}{\sum_{l=1}^{L} P_{J_l}[n]\hat{h}_{J_lR_{m+1}}[n] + 1}\right), \quad m = 1, \ldots, M-1, n \in \mathcal{N}, \tag{9}$$

and the achievable rate of eavesdropping link R-to-E_k in bps/Hz at time slot n can be written as

$$R_{R_mE_k}[n] = \log_2\left(1 + \frac{P_{R_m}[n]\hat{h}_{R_mE_k}[n]}{\sum_{l=1}^{L} P_{J_l}[n]\hat{h}_{J_lE_k}[n] + 1}\right), \quad m \in \mathcal{M}, l \in \mathcal{L}, k \in \mathcal{K}, n \in \mathcal{N}. \tag{10}$$

We assume that the processing duration at RUAV is one slot [6], and following the information-causality constraint for RUAV, only the data received can be forwarded. Therefore, the rate of RUAV at each slot n should satisfy the constraints as follows

$$\sum_{i=2}^{n} R_{R_1R_2}[i] \leq \sum_{i=1}^{n} R_{SR_1}[i], n = 2, \ldots, N, \tag{11a}$$

$$\sum_{i=2}^{n} R_{R_mR_{m+1}}[i] \leq \sum_{i=1}^{n} R_{R_{m-1}R_m}[i], \quad n = 2, \ldots, N, m = 2, \ldots, M-1, \tag{11b}$$

$$\sum_{i=2}^{n} R_{R_MD}[i] \leq \sum_{i=1}^{n} R_{R_{M-1}R_M}[i], n = 2, \ldots, N. \tag{11c}$$

The secrecy rate in a DF multi-hop relay system depends on the weakest link. Therefore, we measure the system secrecy performance by minimum achievable secrecy rate (MASR), which denotes the minimum secrecy throughput among relay links over N slots

$$MASR = \min_{m \in \mathcal{M}} \left\{ \sum_{n=1}^{N} R_{R_m}^{sec}[n], \sum_{n=1}^{N} R_{SR_1}[n] \right\}, \tag{12}$$

where $R_{R_m}^{sec}$ denotes the secrecy rate of R_m-to-R_{m+1} link or R_M-to-D link at time slot n given by

$$R_{R_m}^{sec}[n] = \begin{cases} \left[R_{R_mR_{m+1}}[n] - R_{R_mE_k}[n]\right]^+, \\ m = 1, \ldots, M-1, \\ \left[R_{R_MD}[n] - R_{R_ME_k}[n]\right]^+, \\ m = M, \end{cases} \tag{13}$$

with the operation $[x]^+ \triangleq \max(x, 0)$.

In general, UAV energy consumption is composed of two main components, namely communication-related energy and propulsion energy. Note that in practice, UAV energy consumption caused by communications is much lower than that caused by propulsion. So, the communication energy consumption of UAV can be ignored compared with UAV propulsion energy consumption. As derived in [17], denote the velocity of UAV j at time slot n as $\mathbf{V}_j[n] = (\mathbf{q}_j[n+1] - \mathbf{q}_j[n])/\delta$, where $j \in \{\mathcal{J}, \mathcal{R}\}, n = 1, \cdots, N-1$. Then the total propulsion energy consumption (PSE) [18] of rotary-wing RUAV or JUAV over N time slots can be given by

$$E_j = \sum_{n=1}^{N-1} P_0\left(1 + \frac{3\|\mathbf{V}_j[n]\|^2}{U_{tip}^2}\right) + \frac{1}{2}d_r\rho s\|\mathbf{V}_j[n]\|^3 + P_i\left(\sqrt{1 + \frac{\|\mathbf{V}_j[n]\|^4}{4v_0^4}} - \frac{\|\mathbf{V}_j[n]\|^2}{2v_0^2}\right)^{\frac{1}{2}}, \tag{14}$$

where P_0 and P_i are two constants representing the blade profile power and induced power in hovering status, respectively, U_{tip} denotes the tip speed of the rotor blade, v_0 denotes the mean rotor induced velocity in hover, d_r and s are the fuselage drag ratio and rotor solidity, respectively.

B. PROBLEM FORMULATION

Taking the mobility constraints, power constraints, and information-causality constraints into account, we aim to maximize the minimum secrecy energy efficiency (MSEE) by optimizing the flight trajectory and transmit power of the UAV swarm over all time slots. The optimization problem is formulated as

(P1) :

$$\max_{\mathbf{Q}_R, \mathbf{Q}_J, P_R, P_J} \frac{MASR}{\sum_{l=1}^{L} E_{J_l} + \sum_{m=1}^{M} E_{R_m}} \tag{15}$$

$$\text{s.t. } \|\mathbf{q}_j[n+1] - \mathbf{q}_j[n]\|^2 \leq (V_{max}\delta)^2, \quad j \in \{\mathcal{R}, \mathcal{J}\}, n = 1, \ldots, N-1, \tag{16a}$$

$$\mathbf{q}_j[1] = \mathbf{q}_{j_0}, \mathbf{q}_j[N] = \mathbf{q}_{j_F}, j \in \{\mathcal{R}, \mathcal{J}\}, \tag{16b}$$

$$0 \leq P_{R_m}[n] \leq P_{R_{max}}, n \in \mathcal{N}, m \in \mathcal{M}, \tag{17a}$$

$$0 \leq P_{J_l}[n] \leq P_{J_{max}}, n \in \mathcal{N}, l \in \mathcal{L}, \tag{17b}$$

$$\sum_{i=2}^{n} R_{R_1R_2}[i] \leq \sum_{i=1}^{n} R_{SR_1}[i], i = 2, \ldots, N, \tag{18a}$$

$$\sum_{i=2}^{n} R_{R_mR_{m+1}}[i] \leq \sum_{i=1}^{n} R_{R_{m-1}R_m}[i], \quad i = 2, \ldots, N, m = 2, \ldots, M-1, \tag{18b}$$

$$\sum_{i=2}^{n} R_{R_MD}[i] \leq \sum_{i=1}^{n} R_{R_{M-1}R_M}[i], i = 2, \ldots, N. \tag{18c}$$

It is challenging to solve problem (P1) due to the following four main reasons. First, the operator $[\cdot]^+$ in (13) makes the objective function non-smooth at zero value. Second, both the numerator and the denominator of the objective function are non-concave with respect to $\mathbf{Q}_R$, $\mathbf{Q}_J$, $\mathbf{P}_R$ or $\mathbf{P}_J$, which leads to a non-convex fractional objective function. Third, the information-causality constraint is still a non-convex constraint with respect to all the variables, which makes our problem even more difficult to tackle. Last, both the numerator and the denominator of the fractions in R_{jj^*} and R_{ij} have the trajectory and transmit power optimizing variables, which

are tightly coupled. Therefore, problem (P1) is a non-convex fractional optimization problem, which is difficult to be optimally solved in general.

III. PROPOSED SOLUTION FOR (P1)

In this section, we propose a novel algorithm to solve the non-convex, tightly coupled and complicated optimization problem (P1) by applying block coordinate descent, successive convex approximation techniques, and Dinkelbach method. Firstly, the operation $[\cdot]^+$ in (13) can be omitted by setting $P_{R_m}[n] = 0, m \in \mathcal{M}$, and then problem (P1) is decoupled into four sub-problems: the JUAV's trajectory $\mathbf{Q}_J$ design, the RUAV's trajectory $\mathbf{Q}_R$ design, JUAV's transmit power $\mathbf{P}_J$ control and RUAV's transmit power $\mathbf{P}_R$ control. Finally, the problem (P1) can be solved alternately in an iterative manner until the algorithm converges.

A. OPTIMIZING JUAV'S TRAJECTORY $\mathbf{Q}_J$

Since the work aims to maximize the minimum secrecy energy efficiency, the objective function and constraints in trajectory optimization problem are more complex compared with the previous schemes. For the given RUAV's trajectory $\mathbf{Q}_R$ and the transmit power of UAV swarm $\mathbf{P}_J$, $\mathbf{P}_R$, we can derive the following JUAV's trajectory $\mathbf{Q}_J$ optimization sub-problem (P2):

$$(\text{P2}): \max_{\mathbf{Q}_J} \frac{MASR}{\sum_{l=1}^{L} E_{J_l} + E_R^{total}} \tag{19}$$

$$\text{s.t. } (11),$$

$$\left\|\mathbf{q}_{J_l}[n+1] - \mathbf{q}_{J_l}[n]\right\|^2 \le (V_{max}\delta)^2, l \in \mathcal{L}, n = 1, \ldots, N-1, \tag{20a}$$

$$\mathbf{q}_{J_l}[1] = \mathbf{q}_{J_{l_0}}, \mathbf{q}_{J_l}[N] = \mathbf{q}_{J_{l_F}}, l \in \mathcal{L}. \tag{20b}$$

First, in the complicated fractional objective function (19), the denominator is non-convex due to the third term of E_{J_l}. By introducing auxiliary variables $\phi_J[n] = \{\varphi_{J_l}[n], n = 1, \cdots, N-1, l \in \mathcal{L}\}$, we have the following equation $\varphi_{J_l}^2[n] = \sqrt{1 + \|\mathbf{V}_{J_l}[n]\|^4/4v_0^4} - \|\mathbf{V}_{J_l}[n]\|^2/2v_0^2$, which is equivalent to $\varphi_{J_l}^{-2}[n] = \varphi_{J_l}^2[n] + \|\mathbf{V}_{J_l}[n]\|^2/v_0^2$, so E_{J_l} can be equivalently written as expression (21) with additional constraint (22) as follows

$$\tilde{E}_{J_l} = \sum_{n=1}^{N-1} P_0\left(1 + \frac{3\|\mathbf{V}_{J_l}[n]\|^2}{U_{tip}^2}\right) + \frac{1}{2}d_r\rho s\|\mathbf{V}_{J_l}[n]\|^3 + P_i\varphi_{J_l}[n], \tag{21}$$

$$\varphi_{J_l}^{-2}[n] \le \varphi_{J_l}^2[n] + \|\mathbf{q}_{J_l}[n+1] - \mathbf{q}_{J_l}[n]\|^2/v_0^2, \quad l \in \mathcal{L}, n = 1, \cdots, N-1. \tag{22}$$

By introducing slack variables $\{\eta, \mathbf{z}[n] = \{z_m[n],\}, \Gamma[n] = \{\Gamma_m[n]\}, \mathbf{S} = \{s_l[n] = \|\mathbf{q}_{J_l}[n] - \mathbf{w}_D\|^2 + H^2\}, \mathbf{V} = \{v_{m,l}[n] = \|\mathbf{q}_{J_l}[n] - \mathbf{q}_{R_m}[n]\|^2\}, \mathbf{U} = \{u_{l,k}[n] = \|\mathbf{q}_{J_l}[n] - \mathbf{w}_{E_k}\|^2 + H^2\}\}$, where $l \in \mathcal{L}$, $m \in \mathcal{M}, k \in \mathcal{K}, n \in \mathcal{N}$, problem (P2.1) can be expressed as

$$(\text{P2.1}): \max_{\substack{\mathbf{Q}_J,\varphi_J,\eta,\mathbf{z}[n],\\ \Gamma[n],\mathbf{S},\mathbf{V},\mathbf{U}}} \frac{\eta}{\sum_{l=1}^{L}\tilde{E}_{J_l} + E_R^{total}} \tag{23}$$

$$\text{s.t. } (20)(22),$$

$$\eta \le \sum_{n=1}^{N} z_m[n] - \Gamma_m[n], \forall m, n, \tag{24}$$

$$\sum_{i=2}^{n} z_1[i] \le \sum_{i=1}^{n} R_{SR_1}^{Q_J}[i], n = 2, \cdots, N, \tag{25a}$$

$$\sum_{i=2}^{n} z_m[i] \le \sum_{i=1}^{n} z_{m-1}[i], n = 2, \cdots, N, \quad m = 2, \cdots, M, \tag{25b}$$

$$z_m[n] \le R_{R_mR_{m+1}}^{Q_J}[n], \forall n, m = 1, \cdots, M-1, \tag{26a}$$

$$z_M[n] \le R_{R_MD}^{Q_J}[n], \forall n, \tag{26b}$$

$$\Gamma_m[n] \ge R_{R_mE_k}^{Q_J}[n], \forall m, k, n, \tag{27}$$

$$s_l[n] - \|\mathbf{q}_{J_l}[n] - \mathbf{w}_D\|^2 - H^2 \le 0, \forall n, l, \tag{28}$$

$$\|\mathbf{q}_{J_l}[n] - \mathbf{w}_{E_k}\|^2 + H^2 - u_{l,k}[n] \le 0, \forall n, l, k, \tag{29}$$

$$v_{m,l}[n] - \|\mathbf{q}_{J_l}[n] - \mathbf{q}_{R_m}[n]\|^2 \le 0, \forall n, l, m, \tag{30}$$

where $R_{SR_1}^{Q_J}[n] = \log_2\left(1 + \frac{cs_n}{\sum_L P_{J_l}[n]\gamma_0/v_{1,l}[n]+1}\right)$, $R_{R_mR_{m+1}}^{Q_J}[n] = \log_2\left(1 + \frac{c_{m,n}}{\sum_L P_{J_l}[n]\gamma_0/v_{m+1,l}[n]+1}\right), m = 1, \ldots, M-1, R_{R_MD}^{Q_J}[n] = \log_2\left(1 + \frac{c_{M,n}}{\sum_L P_{J_l}[n]\gamma_0/s_l[n]+1}\right)$, $R_{R_mE_k}^{Q_J}[n] = \log_2\left(1 + \frac{e_{m,k,n}}{\sum_L P_{J_l}[n]\gamma_0/u_{l,k}[n]+1}\right), \forall m, k, n$, and $cs_n = P_S\hat{h}_{SR_1}[n], c_{m,n} = P_{R_m}[n]\hat{h}_{R_mR_{m+1}}[n], c_{M,n} = P_{R_M}[n]\hat{h}_{R_MD}[n], e_{m,k,n} = P_{R_m}[n]\hat{h}_{R_mE_k}[n], \forall m, k, n$.

It can be verified that at the optimal solution to problem (P2), constraints (28)-(30) must hold with equality. If not, $u_{l,k}[n]$ can be further decreased to improve the objective value and then $s_l[n], v_{m,l}[n]$ can also be increased to relax constraints (28) and (30), which means (P2.1) can be further optimized. The optimal value of (P2) is lower bounded by that of (P2.1) owing to slack variable η. However, (P2.1) is still a non-convex optimization problem due to the non-convexity of $R_{R_mE_k}^{Q_J}$ and the right-hand side of (22). Next, the successive convex approximation technique (SCA) is employed to tackle the non-convexity in (22), (27), (28) and (30). Define $\mathbf{Q}_{J_l}^r = \left\{\mathbf{q}_{J_l}^r[n], n \in \mathcal{N}\right\}$ as a given initial trajectory of JUAV l in the r+1-th iteration, $R_{R_mE_k}[n]$ can be replaced by its respective concave upper bound at a given local point [28] as follows

$$R_{R_mE_k}^{Q_J}[n] = \log_2\left(1 + \frac{e_{m,k,n}}{\sum_{l=1}^{L}\frac{P_{J_l}[n]\gamma_0}{u_{l,k}[n]} + 1}\right)$$

$$\leq \sum_{l=1}^{L} W_{m,l,k}^{r}[n]\left(u_{l,k}[n]-u_{l,k}^{r}[n]\right)+X_{m,k}^{r}[n] = R_{R_m E_k}^{Q_J(ub)}[n], \tag{31}$$

where $W_{m,l,k}^{r}[n]=\frac{e_{m,k,n}P_{J_l}[n]\gamma_0}{u_{l,k}^{r}{}^2[n]\left(\sum_L \frac{P_{J_l}[n]\gamma_0}{u_{l,k}^{r}[n]}+1+e_{m,k,n}\right)\left(\sum_L \frac{P_{J_l}[n]\gamma_0}{u_{l,k}^{r}[n]}+1\right)}$, $X_{m,k}^{r}[n]=\log_2\left(1+\frac{e_{m,k,n}}{\sum_L \frac{P_{J_l}[n]\gamma_0}{u_{l,k}^{r}[n]}+1}\right)$, $u_{l,k}^{r}[n]=\|\mathbf{q}_{J_l}^{r}[n]-\mathbf{w}_{E_k}\|^2+H^2$. Similarly, constraints (28) and (30) can be rewritten as

$$s_l[n]+\|\mathbf{q}_{J_l}^{r}[n]\|^2-2\left(\mathbf{q}_{J_l}^{r}[n]-\mathbf{w}_D\right)^T\mathbf{q}_{J_l}[n]-\|\mathbf{w}_D\|^2-H^2\leq 0,\forall n,l, \tag{32}$$

$$v_{m,l}[n]+\|\mathbf{q}_{J_l}^{r}[n]\|^2-2\left(\mathbf{q}_{J_l}^{r}[n]-\mathbf{q}_{R_m}[n]\right)^T\mathbf{q}_{J_l}[n]-\|\mathbf{q}_{R_m}[n]\|^2\leq 0,\forall n,l,m. \tag{33}$$

For right-hand side of (22), the Taylor expansion of multi-variable function is leveraged to obtain a global lower bound, so (22) can be replaced by

$$\varphi_{J_l}^{-2}[n]\leq \varphi_{J_l}^{r}{}^2[n]+2\varphi_{J_l}^{r}[n]\left(\varphi_{J_l}[n]-\varphi_{J_l}^{r}[n]\right)-\|\mathbf{q}_{J_l}^{r}[n+1]-\mathbf{q}_{J_l}^{r}[n]\|^2/v_0^2+2\left(\mathbf{q}_{J_l}^{r}[n+1]-\mathbf{q}_{J_l}^{r}[n]\right)^T\left(\mathbf{q}_{J_l}[n+1]-\mathbf{q}_{J_l}[n]\right)/v_0^2. \tag{34}$$

From the above mathematical transformation, (P2.1) is rewritten as

$$(\text{P2.2}):\max_{\substack{\mathbf{Q}_J,\varphi_J[n],\eta,\mathbf{z}[n],\\ \Gamma[n],\mathbf{S},\mathbf{V},\mathbf{U}}}\frac{\eta}{\sum_{l=1}^{L}\tilde{E}_{J_l}+E_R^{total}} \tag{35}$$

$$\text{s.t. (20), (24)}-\text{(26), (29), (32)}-\text{(34)},$$

$$\Gamma_m[n]\geq R_{R_m E_k}^{Q_J(ub)}[n],\forall m,k,n. \tag{36}$$

It can be observed that (P2.2) is a fractional maximization problem with a linear numerator and convex denominator, as well as all convex constraints, which can be solved by Dinkelbach method. Define μ_J^* as the maximum MSEE and $\tilde{E}_{total}=\sum_{l=1}^{L}\tilde{E}_{J_l}+E_R^{total}$. By referring to [29], [30], we have the theorem that the optimal solutions of problem (P2.2) achieve the maximum MSEE value if and only if $\max_{\mathbf{Q}_J,\varphi_J,\eta,\mathbf{z}[n],\Gamma[n],\mathbf{S},\mathbf{V},\mathbf{U}}\eta-\mu^*\tilde{E}_{total}=0$. For a given MSEE μ_J^*, we can formulate an optimization problem derived from (P2.2) as

$$(\text{P2.3}):\max_{\mathbf{Q}_J,\varphi_J,\eta,\mathbf{z}[n],\Gamma[n],\mathbf{S},\mathbf{V},\mathbf{U}}\eta-\mu^*\tilde{E}_{total} \tag{37}$$

$$\text{s.t. (20), (24)}-\text{(26), (29), (32)}-\text{(34), (36)}.$$

(P2.3) is a convex optimization problem which can be efficiently solved by CVX [31]. Thus, (P2.1) can be solved by an iterative algorithm based on SCA and Dinkelbach method, which is summarized in Algorithm 1.

Algorithm 1 Proposed Iterative Algorithm Based on SCA and Dinkelbach Method for (P2.1)

1: Initialize the maximum tolerance ε, current secrecy energy efficiency ratio μ, UAV's trajectory $\mathbf{Q}_j^r, j\in\{\mathcal{J},\mathcal{R}\}$.
2: **repeat**
3: Solve problem (P2.2) with a given μ, $\mathbf{Q}_j^r$, denote $\left\{\mathbf{Q}_j^*,\varphi_J^*,\eta^*,\mathbf{z}^*[n],\Gamma^*[n],\mathbf{S}^*,\mathbf{V}^*,\mathbf{U}^*\right\}$ as obtained optimal solutions.
4: **if** $\eta^*-\mu\tilde{E}_{total}\leq\varepsilon$ **then**
5: Convergence=**true**.
6: **Output** $\left\{\mu^*,\mathbf{Q}_j^*,\varphi_J^*,\eta^*,\mathbf{z}^*[n],\Gamma^*[n],\mathbf{S}^*,\mathbf{V}^*,\mathbf{U}^*\right\}$
7: **else**
8: Set $\mu^*=\frac{\eta^*}{\tilde{E}_{total}}$, $\mu=\mu^*$,
9: Convergence=**False**
10: **end if**
11: **until** Convergence=**true**.

B. OPTIMIZING RUAV'S TRAJECTORY $\mathbf{Q}_R$

For given JUAV's trajectory $\mathbf{Q}_J$ and transmit power $\mathbf{P}_R$, $\mathbf{P}_J$, we can derive the following sub-problem on the RUAV's trajectory (P3):

$$(\text{P3}):\max_{\mathbf{Q}_R}\frac{MASR}{\sum_{m=1}^{M}E_{R_m}+E_J^{total}} \tag{38}$$

$$\text{s.t. (11)},$$

$$\|\mathbf{q}_{R_m}[n+1]-\mathbf{q}_{R_m}[n]\|^2\leq(V_{max}\delta_t)^2,m\in\mathcal{M},n=1,\ldots,N-1, \tag{39a}$$

$$\mathbf{q}_{R_m}[1]=\mathbf{q}_{R_{m_0}},\mathbf{q}_{R_m}[N]=\mathbf{q}_{R_{m_F}},m\in\mathcal{M}. \tag{39b}$$

Then, introducing $\phi_R=\{\varphi_{R_m}[n],n=1,\ldots,N,m\in\mathcal{M}\}$, we rewrite E_{R_m} in (38) as (40) with additional constraint (41).

$$\tilde{E}_{R_m}=\sum_{n=1}^{N-1}P_0\left(1+\frac{3\|\mathbf{V}_{R_m}[n]\|^2}{U_{tip}^2}\right)+\frac{1}{2}d_r\rho s\|\mathbf{V}_{R_m}[n]\|^3+P_i\varphi_{R_m}[n], \tag{40}$$

$$\varphi_{R_m}^{-2}[n]\leq\varphi_{R_m}^{2}[n]+\|\mathbf{q}_{R_m}[n+1]-\mathbf{q}_{R_m}[n]\|^2/v_0^2,\quad m\in\mathcal{M},n=1,\cdots,N-1. \tag{41}$$

However, (P3) is still a non-convex problem with non-concave objective function and non-convex constraint (11). In particular, the RUAV's trajectory $\mathbf{Q}_R$ exists in both numerator and denominator of the secrecy rate function, which makes our problem (P3) hard to tackle.

First, we introduce slack variables $\{\mathbf{z}[n]=\{z_m[n]\},\Gamma[n]=\{\Gamma_m[n]\},\mathbf{X}_s=\{x_s[n],n\in\mathcal{N}\},\mathbf{Y}_s=\{y_s[n]\},\mathbf{X}_R=\{x_{R_m}[n]\},\mathbf{Y}_R=\{y_{R_m}[n]\},\{\mathbf{S}_{RE}=S_{m,k}[n]\}\}$, where $n\in\mathcal{N},m\in\mathcal{M},k\in\mathcal{K}$. Then, we reformulate (P3) as

$$(\text{P3.1}):\max_{\substack{\mathbf{Q}_R,\eta,\varphi_R,\mathbf{z}[n],\Gamma[n],\\ \mathbf{X}_s,\mathbf{X}_R,\mathbf{Y}_s,\mathbf{Y}_R}}\frac{\eta}{\sum_{m=1}^{M}\tilde{E}_{R_m}+E_J^{total}} \tag{42}$$

s.t. (39) , (41) ,

$$\eta \le \sum_{n=1}^{N} z_m[n] - \Gamma_m[n], \forall m, n, \tag{43}$$

$$\sum_{i=2}^{n} z_1[i] \le \sum_{i=1}^{n} \frac{1}{\ln 2}\left(x_s[i] - y_s[i]\right), \quad n = 2, \cdots, N, \tag{44a}$$

$$\sum_{i=2}^{n} z_m[i] \le \sum_{i=1}^{n} z_{m-1}[i], n = 2, \cdots, N, \quad m = 2, \cdots, M, \tag{44b}$$

$$z_m[n] \le \frac{1}{\ln 2}\left(x_{R_m}[n] - y_{R_m}[n]\right), \forall n, m, \tag{44c}$$

$$P_S \hat{h}_{SR_1}[n] + \sum_{l=1}^{L} P_{J_l}[n]\hat{h}_{J_l R_1}[n] + 1 \ge e^{x_s[n]}, \tag{45a}$$

$$P_{R_m}[n]\hat{h}_{R_m R_{m+1}}[n] + \sum_{l=1}^{L} P_{J_l}[n]\hat{h}_{J_l R_{m+1}}[n] + 1 \ge e^{x_m[n]}, m = 1, \ldots, M-1, \tag{45b}$$

$$P_{R_M}[n]\hat{h}_{R_M D}[n] + \sum_{l=1}^{L} P_{J_l}[n]\hat{h}_{J_l D}[n] + 1 \ge e^{x_M[n]}, \tag{45c}$$

$$\sum_{l=1}^{L} P_{J_l}[n]\hat{h}_{J_l R_1}[n] + 1 \le e^{y_s[n]}, \tag{45d}$$

$$\sum_{l=1}^{L} P_{J_l}[n]\hat{h}_{J_l R_{m+1}}[n] + 1 \le e^{y_{R_m}[n]}, \quad m = 1, \ldots M-1, \tag{45e}$$

$$\sum_{l=1}^{L} P_{J_l}[n]\hat{h}_{J_l D}[n] + 1 \le e^{y_{R_M}[n]}, \tag{45f}$$

$$\Gamma_m[n] \ge \log_2\left(1 + \frac{P_{R_m}[n]\gamma_0}{f_{l,k,n}\left(H^2 + S_{m,k}[n]\right)}\right), \quad \forall m, k, n, \tag{46a}$$

$$S_{m,k}[n] \le \|\mathbf{q}_{R_m}[n] - \mathbf{w}_{E_k}\|^2, \forall m, k, n, \tag{46b}$$

where $f_{l,k,n} = \sum_L \frac{P_{J_l}[n]\gamma_0}{\|\mathbf{q}_{J_l}[n] - \mathbf{w}_{E_k}\|^2 + H^2} + 1$.

After transformation, the problem (P3.1) is still a non-convex problem with non-convex constraints (41), (45) and (46b). Similar to the analysis in (P2), (45) and (46) must hold with equality at the optimal solution and the objective value of (P3.1) gives a lower bound to that of the problem (P3). To handle the non-convex constraints, we define $\mathbf{Q}_{R_m}^r = \left\{\mathbf{q}_{R_m}^r[n], n \in \mathcal{N}\right\}$ as a given initial trajectory of RUAV m in the r+*1*-th iteration.

By applying the first-order Taylor expansion at a given local point $\|\mathbf{q}_{R_m}^r - \mathbf{w}_{E_k}\|^2$, constraint (46b) can be replaced by convex constraint (47).

$$S_{m,k}[n] \le \|\mathbf{q}_{R_m}^r[n] - \mathbf{w}_{E_k}\|^2 + 2\left(\mathbf{q}_{R_m}^r[n] - \mathbf{w}_{E_k}\right)^T \left(\mathbf{q}_{R_m}[n] - \mathbf{q}_{R_m}^r[n]\right). \tag{47}$$

Meanwhile, constraint (41) can be replaced by (48).

$$\begin{aligned}\varphi_{R_m}^{-2}[n] \le\ & \varphi_{R_m}^{r\ 2}[n] + 2\varphi_{R_m}^r[n]\left(\varphi_{R_m}[n] - \varphi_{R_m}^r[n]\right) \\ & - \|\mathbf{q}_{R_m}^r[n+1] - \mathbf{q}_{R_m}^r[n]\|^2 / v_0^2 \\ & + 2\left(\mathbf{q}_{R_m}^r[n+1] - \mathbf{q}_{R_m}^r[n]\right)^T \\ & \left(\mathbf{q}_{R_m}[n+1] - \mathbf{q}_{R_m}[n]\right) / v_0^2.\end{aligned} \tag{48}$$

It can be seen that $\hat{h}_{R_m\Lambda}[n]$ is a convex function of the corresponding norm term $\|\mathbf{q}_{R_m} - \mathbf{q}_\Lambda\|^2$, where Λ can be replaced by S, D, J_l, or R_{m^*}. Thus, the first-order Taylor expansion can be applied to constraints (45a)-(45c), and then the convex lower bound of $\hat{h}_{R_m\Lambda}[n]$ can be expressed as

$$\begin{aligned}\hat{h}_{SR_1}[n] &= \frac{\gamma_0}{\|\mathbf{q}_{R_1}[n] - \mathbf{w}_S\|^2 + H^2} \ge \hat{h}_{SR_1}^{lb}[n] \\ &= \frac{2\gamma_0}{\|\mathbf{q}_{R_1}^r[n] - \mathbf{w}_S\|^2 + H^2} \\ &\quad - \frac{\gamma_0\left(\|\mathbf{q}_{R_1}[n] - \mathbf{w}_S\|^2 + H^2\right)}{\left(\|\mathbf{q}_{R_1}^r[n] - \mathbf{w}_S\|^2 + H^2\right)^2},\end{aligned} \tag{49a}$$

$$\begin{aligned}\hat{h}_{R_m R_{m+1}}[n] &= \frac{\gamma_0}{\|\mathbf{q}_{R_m}[n] - \mathbf{q}_{R_{m+1}}[n]\|^2} \ge \hat{h}_{R_m R_{m+1}}^{lb}[n] \\ &= \frac{2\gamma_0}{\|\mathbf{q}_{R_m}^r[n] - \mathbf{q}_{R_{m+1}}^r[n]\|^2} \\ &\quad - \frac{\gamma_0\left(\|\mathbf{q}_{R_m}[n] - \mathbf{q}_{R_{m+1}[n]}\|^2\right)}{\left(\|\mathbf{q}_{R_m}^r[n] - \mathbf{q}_{R_{m+1}}^r[n]\|^2\right)^2},\end{aligned} \tag{49b}$$

$$\begin{aligned}\hat{h}_{J_l R_m}[n] &= \frac{\gamma_0}{\|\mathbf{q}_{R_m}[n] - \mathbf{q}_{J_l}[n]\|^2} \ge \hat{h}_{J_l R_m}^{lb}[n] \\ &= \frac{2\gamma_0}{\|\mathbf{q}_{R_m}^r[n] - \mathbf{q}_{J_l}[n]\|^2} \\ &\quad - \frac{\gamma_0\left(\|\mathbf{q}_{R_m}[n] - \mathbf{q}_{J_l}[n]\|^2\right)}{\left(\|\mathbf{q}_{R_m}^r[n] - \mathbf{q}_{J_l}[n]\|^2\right)^2},\end{aligned} \tag{49c}$$

$$\begin{aligned}\hat{h}_{R_M D}[n] &= \frac{\gamma_0}{\|\mathbf{q}_{R_M}[n] - \mathbf{w}_D\|^2 + H^2} \ge \hat{h}_{R_M D}^{lb}[n] \\ &= \frac{2\gamma_0}{\|\mathbf{q}_{R_M}^r[n] - \mathbf{w}_D\|^2 + H^2} \\ &\quad - \frac{\gamma_0\left(\|\mathbf{q}_{R_M}[n] - \mathbf{w}_D\|^2 + H^2\right)}{\left(\|\mathbf{q}_{R_M}^r[n] - \mathbf{w}_D\|^2 + H^2\right)^2}.\end{aligned} \tag{49d}$$

Combining (49) with constants in the original inequalities, we can rewrite (45a)-(45c) as

$$P_S \hat{h}_{SR_1}^{lb}[n] + \sum_{l=1}^{L} P_{J_l}[n]\hat{h}_{J_l R_1}^{lb}[n] + 1 \ge e^{x_s[n]}, \tag{50a}$$

$$P_{R_m}[n]\hat{h}^{lb}_{R_mR_{m+1}}[n]+\sum_{l=1}^{L}P_{J_l}[n]\hat{h}^{lb}_{J_lR_{m+1}}[n]+1 \geq e^{x_m[n]},\ m=1,\ldots,M-1, \tag{50b}$$

$$P_{R_M}[n]\hat{h}^{lb}_{R_MD}[n]+\sum_{l=1}^{L}P_{J_l}[n]\hat{h}^{lb}_{J_lD}[n]+1 \geq e^{x_M[n]}. \tag{50c}$$

Here, constraint (50) is jointly concave with respect to optimization variables $\mathbf{q}_{R_m}[n]$, $x_s[n]$ and $x_{R_m}[n]$. By introducing slack variables $\Omega=\{\omega_{R_mJ_l}[n]=\|\mathbf{q}_{R_m}[n]-\mathbf{q}_{J_l}[n]\|^2, l\in\mathcal{L}, m\in\mathcal{M}, n\in\mathcal{N}\}$, we can transform constraints (45d)-(45e) into the following inequalities.

$$\gamma_0\sum_{l=1}^{L}\frac{P_{J_l}[n]}{\omega_{R_1J_l}[n]}+1\leq e^{y_s[n]}, \tag{51a}$$

$$\|\mathbf{q}_{R_1}[n]-\mathbf{q}_{J_l}[n]\|^2-\omega_{R_1J_l}\geq 0, \tag{51b}$$

$$\gamma_0\sum_{l=1}^{L}\frac{P_{J_l}[n]}{\omega_{R_{m+1}J_l}[n]}+1\leq e^{y_{R_m}[n]}, \tag{51c}$$

$$\|\mathbf{q}_{R_{m+1}}[n]-\mathbf{q}_{J_l}[n]\|^2-\omega_{R_{m+1}J_l}\geq 0,\ m=1,\ldots,M-1. \tag{51d}$$

At the optimal value of (P3.1), (51b) and (51d) must hold with equality. Besides, $\omega_{R_mJ_l}$ can be increased to relax constraints (51a) and (51c), which will further relax original constraints (45d)-(45e). However, though (45d)-(45e) has been transformed, (51) and (45f) are still non-convex. We apply successive convex approximation technique utilizing the following inequalities.

$$\gamma_0\sum_{l=1}^{L}\frac{P_{J_l}[n]}{\omega_{R_1J_l}[n]}+1\geq e^{y_s^r[n]}\left(y_s[n]-y_s^r[n]+1\right), \tag{52a}$$

$$\gamma_0\sum_{l=1}^{L}\frac{P_{J_l}[n]}{\omega_{R_{m+1}J_l}[n]}+1\geq e^{y^r_{R_m}[n]}\left(y_{R_m}[n]-y^r_{R_m}[n]\right)+e^{y^r_{R_m}[n]},\ m=1,\ldots,M-1, \tag{52b}$$

$$\gamma_0\sum_{l=1}^{L}\frac{P_{J_l}[n]}{\|\mathbf{q}_{J_l}[n]-\mathbf{w}_D\|^2}+1\geq e^{y^r_{R_M}[n]}y_{R_M}[n]+e^{y^r_{R_M}[n]}-e^{y^r_{R_M}[n]}y^r_{R_M}[n], \tag{52c}$$

$$\omega_{R_mJ_l}[n]\leq 2\left(\mathbf{q}^r_{R_m}[n]-\mathbf{q}_{J_l}[n]\right)^T\left(\mathbf{q}_{R_m}[n]-\mathbf{q}^r_{R_m}[n]\right)+\|\mathbf{q}^r_{R_m}[n]-\mathbf{q}_{J_l}[n]\|^2. \tag{52d}$$

According to the above transformation, the constraints in (P3.1) can be replaced by transformed convex constraints and (P3.1) is therefore reformulated as

$$\text{(P3.2)}: \max_{\Upsilon}\frac{\eta}{\sum_{m=1}^{M}\tilde{E}_{R_m}+E_J^{total}} \quad \text{s.t. (39), (43), (44), (46}a\text{), (47), (48), (50), (52),} \tag{53}$$

where $\Upsilon=\{\mathbf{Q}_R,\eta,\varphi_R,\mathbf{z}[n],\Gamma[n],\mathbf{X}_s,\mathbf{X}_R,\mathbf{Y}_s,\mathbf{Y}_R,\Omega\}$. It can be seen that (P3.2) is a fractional maximization problem with a linear numerator and convex denominator, as well as all convex constraints. We define μ_R^* as the maximum MSEE and $\tilde{E}_{total}=\sum_{m=1}^{M}\tilde{E}_{R_m}+E_J^{total}$, and then, we can formulate an optimization problem derived from (P3.2) as

$$\text{(P3.3)}: \max_{\Upsilon}\eta-\mu_R^*\tilde{E}_{total} \quad \text{s.t. (39), (43), (44), (46}a\text{), (47), (48), (50), (52),} \tag{54}$$

After the above approximation, (P3.3) is a convex optimization problem which can be efficiently solved by CVX. Thus, (P3.1) can be solved by an iterative algorithm based on SCA and Dinkelbach method, which is similar to Algorithm 1.

C. Optimizing JUAV'S TRANSMIT POWER $\mathbf{P}_J$

Knowing the JUAV's trajectory $\mathbf{Q}_J$, the RUAV's trajectory $\mathbf{Q}_R$ and the RUAV's transmit power $\mathbf{P}_R$, we can formulate the sub-problem (P4) as

$$\text{(P4)}: \max_{\mathbf{P}_J}\frac{MASR}{E^{total}} \quad \text{s.t. (4) (9)}, \tag{55}$$

where $E^{total}=\sum_{l=1}^{L}E_{J_l}+\sum_{m=1}^{M}E_{R_m}$. Since the propulsion energy of UAV is independent of the UAV's transmit power, E^{total} is a constant and (P4) is easier to solve compared with the previous sub-problems. Therefore, we introduce slack variables $\{\eta,\Gamma[n]=\{\Gamma_m[n]\}\}$ and reformulate problem (P4) as

$$\text{(P4.1)}: \max_{\mathbf{P}_J,\eta,\Gamma[n]}\frac{\eta}{E^{total}} \tag{56}$$

$$\text{s.t. (6)},$$

$$\eta\leq\sum_{n=1}^{N}R^{P_J}_{R_mR_{m+1}}[n]-\Gamma_m[n],\ m=1,\ldots,M-1,\forall n, \tag{57a}$$

$$\eta\leq\sum_{n=1}^{N}R^{P_J}_{R_MD}[n]-\Gamma_M[n],\forall n, \tag{57b}$$

$$\sum_{i=2}^{n}R^{P_J}_{R_1R_2}[i]\leq\sum_{i=1}^{n}R^{P_J}_{SR_1}[i],\ n=2,\cdots,N, \tag{58a}$$

$$\sum_{i=2}^{n}R^{P_J}_{R_mR_{m+1}}[i]\leq\sum_{i=1}^{n}R^{P_J}_{R_{m-1}R_m}[i],\ n=2,\cdots,N,m=2,\cdots,M-1, \tag{58b}$$

$$\sum_{i=2}^{n}R^{P_J}_{R_MD}[i]\leq\sum_{i=1}^{n}R^{P_J}_{R_{M-1}R_M}[i],\ n=2,\cdots,N, \tag{58c}$$

$$\Gamma_m[n]\geq R^{P_J}_{R_mE_k}[n],\forall m,k,n. \tag{59}$$

(P4.1) is still a non-convex problem with non-convex constraints (57) and (58), and (P4.1) serves as a lower bound to the original problem (P4) owing to slack variable η. Then,

we focus on solving the non-convex constraints in (P4.1). In the following formulation, we denote $P_{J_l}^r[n]$ as the result of JUAV l transmit power after r-th iteration at the time slot n.

We apply successive convex approximation technique on $R_{SR_1}^{P_J}[n]$, $R_{R_mR_{m+1}}^{P_J}[n]$, and $R_{R_mR_D}^{P_J}[n]$ to obtain the convex lower bounds.

$$\begin{aligned} R_{SR_1}^{P_J}[n] &= \log_2\left(1+\frac{cs_n}{\sum_{l=1}^{L} P_{J_l}[n]\hat{h}_{J_lR_1}[n]+1}\right) \\ &\geq \sum_{l=1}^{L} A_l^r[n]\left(P_{J_l}[n]-P_{J_l}^r[n]\right)+B^r[n] \\ &= R_{SR_1}^{P_J(lb)}[n], \end{aligned} \tag{60a}$$

$$\begin{aligned} R_{R_mR_{m+1}}^{P_J}[n] &= \log_2\left(1+\frac{c_{m,n}}{\sum_{L} P_{J_l}[n]\hat{h}_{J_lR_{m+1}}[n]+1}\right) \\ &\geq \sum_{l=1}^{L} C_{l,m}^r[n]\left(P_{J_l}[n]-P_{J_l}^r[n]\right)+D_m^r[n] \\ &= R_{R_mR_{m+1}}^{P_J(lb)}[n], m=1,\ldots,M-1, \end{aligned} \tag{60b}$$

$$\begin{aligned} R_{R_MD}^{P_J}[n] &= \log_2\left(1+\frac{c_{M,n}}{\sum_{l=1}^{L} P_{J_l}[n]\hat{h}_{J_lD}[n]+1}\right) \\ &\geq \sum_{l=1}^{L} C_{l,M}^r[n]\left(P_{J_l}[n]-P_{J_l}^r[n]\right)+D_M^r[n] \\ &= R_{R_MD}^{P_J(lb)}[n], \end{aligned} \tag{60c}$$

where $A^r[n] = \frac{-cs_n\hat{h}_{J_lR_1}[n]/\ln 2}{\left(\sum_L P_{J_l}^r[n]\hat{h}_{J_lR_1}[n]+1+cs_n\right)\left(\sum_L P_{J_l}^r[n]\hat{h}_{J_lR_1}[n]+1\right)}$, $B^r[n] = \log_2\left(1+\frac{cs_n}{\sum_L P_{J_l}^r[n]\hat{h}_{J_lR_1}[n]+1}\right)$, $C_{l,m}^r[n] = \frac{-c_{m,n}\hat{h}_{J_lR_{m+1}}[n]}{\ln 2\left(\sum_L P_{J_l}^r[n]\hat{h}_{J_lR_{m+1}}[n]+1+c_{m,n}\right)\left(\sum_L P_{J_l}^r[n]\hat{h}_{J_lR_{m+1}}[n]+1\right)}$, $D_m^r[n] = \log_2\left(1+\frac{c_{m,n}}{\sum_L P_{J_l}^r[n]\hat{h}_{J_lR_{m+1}}[n]+1}\right)$, $C_{l,M}^r[n] = \frac{-c_{M,n}\hat{h}_{J_lD}[n]}{\ln 2\left(\sum_L P_{J_l}^r[n]\hat{h}_{J_lD}[n]+1+c_{M,n}\right)\left(\sum_L P_{J_l}^r[n]\hat{h}_{J_lD}[n]+1\right)}$, $D_M^r[n] = \log_2\left(1+\frac{c_{M,n}}{\sum_L P_{J_l}^r[n]\hat{h}_{J_lD}[n]+1}\right)$, then the problem (P4.1) can be reformulated as

$$\begin{aligned} (\text{P4.2}) \max_{\mathbf{P}_J,\eta,\Gamma[n]} \ & \frac{\eta}{E^{total}} \\ \text{s.t. } & (6)\ (59)\,, \\ & \eta \leq \sum_{n=1}^{N} R_{R_mR_{m+1}}^{P_J(lb)}[n]-\Gamma_m[n], \\ & m=1,\ldots,M-1,\forall n, \end{aligned} \tag{61}$$

$$\eta \leq \sum_{n=1}^{N} R_{R_MD}^{P_J(lb)}[n]-\Gamma_M[n],\forall n, \tag{62a}$$

$$\sum_{i=2}^{n} R_{R_1R_2}^{P_J}[i] \leq \sum_{i=1}^{n} R_{SR_1}^{P_J(lb)}[i], \quad n=2,\cdots,N, \tag{62b}$$

$$\sum_{i=2}^{n} R_{R_mR_{m+1}}^{P_J}[i] \leq \sum_{i=1}^{n} R_{R_{m-1}R_m}^{P_J(lb)}[i], \quad n=2,\cdots,N, m=2,\cdots,M-1, \tag{63a}$$

$$\sum_{i=2}^{n} R_{R_MD}^{P_J}[i] \leq \sum_{i=1}^{n} R_{R_{M-1}R_M}^{P_J(lb)}[i], \quad n=2,\cdots,N, \tag{63b}$$

$$\sum_{i=2}^{n} R_{R_MD}^{P_J}[i] \leq \sum_{i=1}^{n} R_{R_{M-1}R_M}^{P_J(lb)}[i], \quad n=2,\cdots,N. \tag{63c}$$

By the aforementioned approximation with first-order Taylor expansion, (P4.2) is a convex problem which can be efficiently solved by CVX. It can be seen that the objective value of (P4.1) with the solution obtained by solving (P4.2) is always no less than that with any P_J^r and the optimal value of (P4.2) serves as lower bound for the original problem (P4).

D. OPTIMIZING RUAV'S TRANSMIT POWER $\mathbf{P}_R$

For given $\mathbf{Q}_J$, $\mathbf{Q}_R$, and $\mathbf{P}_J$, the original problem (P1) can be equivalently rewritten as

$$\begin{aligned} (\text{P5}): \max_{\mathbf{P}_R} \ & \frac{MASR}{E^{total}} \\ \text{s.t. } & (5)\ (11)\,. \end{aligned} \tag{64}$$

It is similar to subsection-C that we introduce slack variables $\{\eta, \Gamma[n]=\Gamma_m[n], \forall m,n\}$ to solve the non-concave object function, and reformulate (P5) as

$$\begin{aligned} (\text{P5.1}): \max_{\mathbf{P}_R,\eta,\Gamma[n]} \ & \frac{\eta}{E^{total}} \\ \text{s.t. } & (5)\,, \\ & \eta \leq \sum_{n=1}^{N} R_{R_mR_{m+1}}^{P_R}[n]-\Gamma_m[n], \\ & m=1,\ldots,M-1,\forall n, \end{aligned} \tag{65}$$

$$\eta \leq \sum_{n=1}^{N} R_{R_MD}^{P_R}[n]-\Gamma_m[n],\forall n, \tag{66a}$$

$$\sum_{i=2}^{n} R_{R_1R_2}^{P_R}[i] \leq \sum_{i=1}^{n} R_{SR_1}^{P_R}[i], \quad n=2,\cdots,N, \tag{66b}$$

$$\sum_{i=2}^{n} R_{R_mR_{m+1}}^{P_R}[i] \leq \sum_{i=1}^{n} R_{R_{m-1}R_m}^{P_R}[i], \quad n=2,\cdots,N, m=2,\cdots,M-1, \tag{67a}$$

$$\sum_{i=2}^{n} R_{R_MD}^{P_R}[i] \leq \sum_{i=1}^{n} R_{R_{M-1}R_M}^{P_R}[i], \quad n=2,\cdots,N, \tag{67b}$$

$$\Gamma_m[n] \geq R_{R_mE_k}^{P_M}[n]\,,\forall m,k,n, \tag{67c}$$

$$\tag{68}$$

where $R_{SR_1}^{P_R}[n]$ is independent with P_R, so it is a constant. And $R_{R_mR_{m+1}}^{P_R}[n] = \log_2\left(1+a_{m,n}P_{R_m}[n]\right)$, $R_{R_MD}^{P_R}[n] = \log_2\left(1+f_nP_{R_M}[n]\right)$, $R_{R_mE_k}^{P_R}[n] = \log_2\left(1+b_{m,k,n}P_{R_m}[n]\right)$,

$a_{m,n} = \frac{\hat{h}_{R_m R_{m+1}}[n]}{\sum_L P_{J_l}[n]\hat{h}_{J_l R_{m+1}}[n]+1}, m = 1,\ldots,M-1, f_n = \frac{\hat{h}_{R_M D}[n]}{\sum_{l=1}^{L} P_{J_l}[n]\hat{h}_{J_l D}[n]+1}, b_{m,k,n} = \frac{\hat{h}_{R_m E_k}[n]}{\sum_{l=1}^{L} P_{J_l}[n]\hat{h}_{J_l E_k}[n]+1}, \forall m,k,n.$

It can be seen that the optimal value of (P5.1) is a lower bound of (P5) owing to slack variable η. However, (P5.1) is still a non-convex problem due to non-convex constraints (67) and (68), which can be solved by the successive convex approximation technique. The given initial transmit power of RUAV m in the r+*1*-th iteration is defined as $P^r_{R_m} = \left\{P^r_{R_m}[n], \forall m, n\right\}$, and then $R^{P_M}_{R_m R_{m+1}}[n], R^{P_M}_{R_M D}[n], R^{P_M}_{R_m E_k}[n]$ can be replaced by respective convex upper bounds as follows

$$\begin{aligned} R^{P_M}_{R_m R_{m+1}}[n] &= \log_2\left(1 + a_{m,n}P_{R_m}[n]\right) \\ &\le G^r_m[n]\left(P_{R_m}[n] - P^r_{R_m}[n]\right) + I^r_m[n] \\ &= R^{P_M(ub)}_{R_m R_{m+1}}[n], \end{aligned} \tag{69a}$$

$$\begin{aligned} R^{P_M}_{R_M D}[n] &= \log_2\left(1 + f_n P_{R_M}[n]\right) \\ &\le G^r_M[n]\left(P_{R_M}[n] - P^r_{R_M}[n]\right) + I^r_M[n] \\ &= R^{P_M(ub)}_{R_M D}[n], \end{aligned} \tag{69b}$$

$$\begin{aligned} R^{P_M}_{R_m E_k}[n] &= \log_2\left(1 + b_{m,k,n}P_{R_m}[n]\right) \\ &\le F^r_m[n]\left(P_{R_m}[n] - P^r_{R_m}[n]\right) + M^r_m[n] \\ &= R^{P_M(ub)}_{R_m E_k}[n], \end{aligned} \tag{69c}$$

where $G^r_m[n] = \frac{a_{m,n}}{\ln 2\left(1+a_{m,n}P^r_{R_m}[n]\right)}$, $I^r_m[n] = \log_2\left(1+a_{m,n}\ P^r_{R_m}\right)$, $m = 1,\ldots,M-1$, $G^r_M[n] = \frac{f_n}{\ln 2\left(1+f_n P^r_{R_M}[n]\right)}$, $F^r_{m,k}[n] = \frac{b_{m,k,n}}{\ln 2\left(1+b_{m,k,n}P^r_{R_m}[n]\right)}$, $I^r_M[n] = \log_2\left(1+f_n P^r_{R_M}\right)$, $M^r_{m,k}[n] = \log_2\left(1+b_{m,k,n}P^r_{R_m}\right)$. we can combine (69a)-(69c) and rewrite (P5.1) as

$$\text{(P5.2)}: \max_{\mathbf{P}_R,\eta,\Gamma[n]} \frac{\eta}{E^{total}} \tag{70}$$

$$\text{s.t. (5) , (66) ,}$$

$$\sum_{i=2}^{n} R^{P_M(ub)}_{R_1 R_2}[i] \le \sum_{i=1}^{n} R_{SR_1}[i], n = 2,\cdots,N, \tag{71a}$$

$$\sum_{i=2}^{n} R^{P_M(ub)}_{R_m R_{m+1}}[i] \le \sum_{i=1}^{n} R^{P_M}_{R_{m-1}R_m}[i], \quad n = 2,\cdots,N, m = 2,\cdots,M-1, \tag{71b}$$

$$\sum_{i=2}^{n} R^{P_M(ub)}_{R_M D}[i] \le \sum_{i=1}^{n} R^{P_M}_{R_{M-1}R_M}[i], \quad n = 2,\cdots,N, \tag{71c}$$

$$\Gamma_m[n] \ge R^{P_M(ub)}_{R_m E_k}[n], \forall m,k,n, \tag{72}$$

(P5.2) is a convex problem with concave objective function and convex constraints, and can be solved by CVX.

E. OVERALL ALGORITHM

Based on the solutions presented in the previous four subsections, we proposed an overall iterative algorithm to solve (P1) by applying the block coordinate descent method [32]. Specifically, we divide the optimization variables of the original problem into four blocks, including JUAV's trajectory $\mathbf{Q}_J$, RUAV's trajectory $\mathbf{Q}_R$, JUAV's transmit power $\mathbf{P}_J$ and RUAV's transmit power $\mathbf{P}_R$. Then, we optimize them by solving (P2.3), (P3.3), (P4.2) and (P5.2) alternately, while keeping the other three variable blocks fixed. Furthermore, the obtained solution in each iteration is used in the next iteration. The details of this algorithm are summarized in Algorithm 2. However, it is worth noting that (P2.3), (P3.3), (P4.2) and (P5.2) are the approximate problems of the subproblems. Thus, the convergence analysis for the classical coordinate descent method cannot be applied directly, so we prove the convergence of Algorithm 2 as follows.

Algorithm 2 Proposed Iterative Algorithm RJPQ for (P1)

1: Initialize JUAV's trajectory $\mathbf{Q}^0_J$, RUAV's trajectory $\mathbf{Q}^0_R$, JUAV's transmit power $\mathbf{P}^0_J$, RUAV's transmit power $\mathbf{P}^0_R$, the minimum threshold value ϵ and iteration times $r = 0$.
2: **repeat**
3: Set $r = r + 1$.
4: Given feasible solution $\left(\mathbf{Q}^{r-1}_J, \mathbf{Q}^{r-1}_R, \mathbf{P}^{r-1}_J, \mathbf{P}^{r-1}_R\right)$, solve problem (P2.3) with Algorithm 1 and obtain corresponding optimal solution $\mathbf{Q}^r_J$, μ_J.
5: Given feasible solution $\left(\mathbf{Q}^r_J, \mathbf{Q}^{r-1}_R, \mathbf{P}^{r-1}_J, \mathbf{P}^{r-1}_R\right)$, solve problem (P3.3) with Algorithm 2 and obtain corresponding optimal solution $\mathbf{Q}^r_R$, μ_R.
6: Given feasible solution $\left(\mathbf{Q}^r_J, \mathbf{Q}^r_R, \mathbf{P}^{r-1}_J, \mathbf{P}^{r-1}_R\right)$, solve problem (P4.2) and obtain corresponding optimal solution $\mathbf{P}^r_J$.
7: Given feasible solution $\left(\mathbf{Q}^r_J, \mathbf{Q}^r_R, \mathbf{P}^r_J, \mathbf{P}^{r-1}_R\right)$, solve problem (P5.2) and obtain corresponding optimal solution $\mathbf{P}^r_R$.
8: Calculate and update objective value in (P1) with current optimal solution.
9: **until** the increase of the objective value in (P1) is less than threshold ϵ.

Define

$$\begin{aligned} \chi^{r(lb)}_{\mathbf{Q}_J}(\mathbf{Q}_J,\mathbf{Q}_R,\mathbf{P}_J,\mathbf{P}_R) &= \chi^r_{\mathbf{Q}_J}, \\ \chi^{r(lb)}_{\mathbf{Q}_R}(\mathbf{Q}_J,\mathbf{Q}_R,\mathbf{P}_J,\mathbf{P}_R) &= \chi^r_{\mathbf{Q}_R}, \\ \chi^{r(lb)}_{\mathbf{P}_J}(\mathbf{Q}_J,\mathbf{Q}_R,\mathbf{P}_J,\mathbf{P}_R) &= \chi^r_{\mathbf{P}_J}, \\ \chi^{r(lb)}_{\mathbf{P}_R}(\mathbf{Q}_J,\mathbf{Q}_R,\mathbf{P}_J,\mathbf{P}_R) &= \chi^r_{\mathbf{P}_R}, \end{aligned}$$

where $\chi^r_{\mathbf{Q}_J}$, $\chi^r_{\mathbf{Q}_R}$, $\chi^r_{\mathbf{P}_J}$ and $\chi^r_{\mathbf{P}_R}$ are objective values of problems (P2.3), (P3.3), (P4.2), and (P5.2) based on $\mathbf{Q}_J$, $\mathbf{Q}_R$, $\mathbf{P}_J$, and $\mathbf{P}_R$. First, in step 4 of Algorithm 2, it follows

$$\begin{aligned} \chi\left(\mathbf{Q}^r_J,\mathbf{Q}^r_R,\mathbf{P}^r_J,\mathbf{P}^r_R\right) &\overset{(a)}{=} \chi^{r(lb)}_{\mathbf{Q}_J}\left(\mathbf{Q}^r_J,\mathbf{Q}^r_R,\mathbf{P}^r_J,\mathbf{P}^r_R\right) \\ &\overset{(b)}{\le} \chi^{r(lb)}_{\mathbf{Q}_J}\left(\mathbf{Q}^{r+1}_J,\mathbf{Q}^r_R,\mathbf{P}^r_J,\mathbf{P}^r_R\right) \\ &\overset{(c)}{\le} \chi\left(\mathbf{Q}^{r+1}_J,\mathbf{Q}^r_R,\mathbf{P}^r_J,\mathbf{P}^r_R\right), \end{aligned} \tag{73}$$

where (a) holds since the first-order Taylor expansions in (31)-(34) are tight at the given local points, respectively, which means that problem (P2.2) at $\mathbf{Q}_J^r$ has the same objective value as problem (P2); (b) holds since in step 4 of Algorithm 2 with given $\mathbf{Q}_R^r$, $\mathbf{P}_J^r$ and $\mathbf{P}_R^r$, problem (P2.3) is solved optimally with solution $\mathbf{Q}_J^{r+1}$; (c) holds since the objective value of problem (P2.3) is the lower bound of its original problem (P2) at $\mathbf{Q}_J^{r+1}$. The inequality in (73) suggests that although only an approximate optimization problem (P2.2) is solved for obtaining the JUAV's trajectory, the objective value of problem (P2) is still non-decreasing after each iteration.

Second, for given $\mathbf{Q}_J^{r+1}$, $\mathbf{P}_J^r$, and $\mathbf{P}_R^r$ in step 5 of Algorithm 2, it follows

$$\begin{aligned}\chi\left(\mathbf{Q}_J^{r+1},\mathbf{Q}_R^r,\mathbf{P}_J^r,\mathbf{P}_R^r\right)&\overset{(d)}{=}\chi_{\mathbf{Q}_R}^{r(lb)}\left(\mathbf{Q}_J^{r+1},\mathbf{Q}_R^r,\mathbf{P}_J^r,\mathbf{P}_R^r\right)\\&\overset{(e)}{\leq}\chi_{\mathbf{Q}_R}^{r(lb)}\left(\mathbf{Q}_J^{r+1},\mathbf{Q}_R^{r+1},\mathbf{P}_J^r,\mathbf{P}_R^r\right)\\&\overset{(f)}{\leq}\chi\left(\mathbf{Q}_J^{r+1},\mathbf{Q}_R^{r+1},\mathbf{P}_J^r,\mathbf{P}_R^r\right),\end{aligned}\tag{74}$$

where (d) holds since the first-order Taylor expansions in (47)-(49) and (52) are tight at given local points, respectively, which means that problem (P3.2) at $\mathbf{Q}_P^r$ has the same objective value as problem (P3); (e) holds since in step 5 of Algorithm 2 with given $\mathbf{Q}_J^{r+1}$, $\mathbf{P}_J^r$, and $\mathbf{P}_R^r$, problem (P3.3) is solved optimally with solution $\mathbf{Q}_P^{r+1}$;(f) holds since the objective value of problem (P3.3) is the lower bound of its original problem (P3) at $\mathbf{Q}_R^{r+1}$. The inequality in (74) suggests that although only an approximate optimization problem (P3.2) is solved for obtaining the RUAV's trajectory, the objective value of problem (P3) is still non-decreasing after each iteration. Next, for the given $\mathbf{Q}_J^{r+1}$, $\mathbf{Q}_R^{r+1}$, and $\mathbf{P}_R^r$ in step 6 of Algorithm 2, it follows

$$\begin{aligned}&\chi\left(\mathbf{Q}_J^{r+1},\mathbf{Q}_R^{r+1},\mathbf{P}_J^r,\mathbf{P}_R^r\right)\\&\quad=\chi_{\mathbf{P}_J}^{r(lb)}\left(\mathbf{Q}_J^{r+1},\mathbf{Q}_R^{r+1},\mathbf{P}_J^r,\mathbf{P}_R^r\right)\\&\quad\leq\chi_{\mathbf{P}_J}^{r(lb)}\left(\mathbf{Q}_J^{r+1},\mathbf{Q}_R^{r+1},\mathbf{P}_J^{r+1},\mathbf{P}_R^r\right)\\&\quad\leq\chi\left(\mathbf{Q}_J^{r+1},\mathbf{Q}_R^{r+1},\mathbf{P}_J^{r+1},\mathbf{P}_R^r\right).\end{aligned}\tag{75}$$

Then, for given $\mathbf{Q}_J^{r+1}$, $\mathbf{Q}_R^{r+1}$, and $\mathbf{P}_J^{r+1}$ in step 7 of Algorithm 2, it follows

$$\begin{aligned}&\chi\left(\mathbf{Q}_J^{r+1},\mathbf{Q}_R^{r+1},\mathbf{P}_J^{r+1},\mathbf{P}_R^r\right)\\&\quad=\chi_{\mathbf{P}_R}^{r(lb)}\left(\mathbf{Q}_J^{r+1},\mathbf{Q}_R^{r+1},\mathbf{P}_J^{r+1},\mathbf{P}_R^r\right)\\&\quad\leq\chi_{\mathbf{P}_R}^{r(lb)}\left(\mathbf{Q}_J^{r+1},\mathbf{Q}_R^{r+1},\mathbf{P}_J^{r+1},\mathbf{P}_R^{r+1}\right)\\&\quad\leq\chi\left(\mathbf{Q}_J^{r+1},\mathbf{Q}_R^{r+1},\mathbf{P}_J^{r+1},\mathbf{P}_R^{r+1}\right).\end{aligned}\tag{76}$$

Based on (73)-(76), we obtain

$$\chi\left(\mathbf{Q}_J^r,\mathbf{Q}_R^r,\mathbf{P}_J^r,\mathbf{P}_R^r\right)\leq\chi\left(\mathbf{Q}_J^{r+1},\mathbf{Q}_R^{r+1},\mathbf{P}_J^{r+1},\mathbf{P}_R^{r+1}\right),\tag{77}$$

which indicates that the objective value of the problem (P1) is non-decreasing after each iteration r of Algorithm 2. Since the objective value of the problem (P1) is upper bounded by a finite value, the proposed Algorithm 2 is guaranteed to converge. Simulation results in Section IV show that the proposed algorithm converges quickly for our considered setup.

In Algorithm 2, each sub-problem can be approximated as a linear problem by taking first-order Taylor expansion. Then the problem (P4) and (P5) can be solved by interior point method with computational complexity $\mathcal{O}\left(\sqrt{\tilde{N}}\log\frac{1}{\varepsilon_0}\right)$, where $\tilde{N}$ denotes the decision variables [19], and ε_0 denotes iterative accuracy [32]. Similarly, the computational complexity of problem (P2) and (P3) are $\mathcal{O}\left(C\sqrt{\tilde{N}}\log\frac{1}{\varepsilon_0}\right)$, where C denotes the iteration numbers for updating μ in Algorithm 1. Thus, the overall computational complexity of Algorithm 2 is $\mathcal{O}(C(\sqrt{((K+3)L+(L+2)M)N+1}\log\frac{1}{\varepsilon_0}))+\mathcal{O}(C(\sqrt{((6+L)M+2)N+1}\log\frac{1}{\varepsilon_0}))+\mathcal{O}(\sqrt{(L+M)N+1}\log\frac{1}{\varepsilon_0})+\mathcal{O}(\sqrt{2MN+1}\log\frac{1}{\varepsilon_0})$.

IV. SIMULATIONS

In this section, we provide numerical results to demonstrate the effectiveness of the proposed scheme. This article attempts to investigate the effectiveness of the cooperative UAV swarm scheme to improve the secrecy energy efficiency performance in a multi-hop mobile relay system, and we therefore choose a basic system model to study the novel scheme, where $M=2, J=1$, and $K=1$. However, the proposed scheme and algorithm can be applied to a more complex case with multiple JUAVs or eavesdroppers. The initial locations and final locations of the UAV swarm are set as $\mathbf{q}_{R_{1_0}}=[350,500]^T$, $\mathbf{q}_{R_{2_0}}=[450,500]^T$, $\mathbf{q}_{R_{1_F}}=[350,-500]^T$, $\mathbf{q}_{R_{2_F}}=[450,-500]^T$, $\mathbf{q}_{J_0}=[200,500]^T$, $\mathbf{q}_{J_F}=[200,-500]^T$. The UAVs' initial UAV trajectories in the proposed and benchmark schemes consist of line-segments connecting their initial locations to final locations. The maximum flying speed of UAV is set as $V_{max}=20m/s$. The flight altitude is set as $H=50m$. Furthermore, locations of ground legitimate users are set as $\mathbf{w}_S=[0,0]^T$ and $\mathbf{w}_D=[600,0]^T$, and the location of the eavesdropper (denoted by E afterwards) is $\mathbf{w}_E=[300,-100]^T$. The receiver noise power is $\sigma^2=-110dBm$ while the channel power gain is $\rho_0=-60dB$ at the reference distance $d_0=1m$. Therefore, the channel gain-to-noise at the reference distance is $\gamma_0=80dB$. The maximum transmit power of the source node is set as $P_S=30dBm$, and the maximum transmit power of both RUAV and JUAV is assumed as $P_{R_{max}}=20dBm$ and $P_{J_{max}}=20dBm$, respectively. The threshold ε in Algorithm 2 is set as 10^{-4}. And other parameters on propulsion energy consumption are referred to [18].

Simulation results demonstrate the effectiveness of the proposed scheme named joint power and trajectory optimization for RUAV and JUAV (denoted by RJPQ). Besides, we introduce the following three benchmark schemes for comparison: trajectory optimization for RUAV and JUAV with fixed transmit power (denoted by RJQ), joint power and trajectory optimization for RUAV with fixed JUAV's trajectory and

power (denoted by RPQ), joint power and trajectory optimization on RUAV without friendly jammer UAV (RPQ/NJ). Especially, in RJQ, we set $P_{J_{max}} = P_{M_{max}} = 20dBm$ and solve (P2.3) and (P3.3) iteratively to optimize flight trajectory of the UAV swarm until convergence. In RPQ, (P3.3) and (P5.2) are solved iteratively until convergence, where the JUAV's trajectory and power are set as the initial settings in the RJPQ scheme. In RPQ/NJ, we set $\mathbf{P}_j = 0$ and then solve (P3) and (P5) iteratively until convergence.

Fig.2 shows the convergence behavior of the proposed Algorithm 2 under $T = 90s$. From Fig.2, it can be observed that the minimum secrecy energy efficiency increases rapidly with the times of iterations increased, and the algorithm converges after about 16 iterations.

In Fig.3, we illustrate the optimized UAV swarm trajectory obtained by the proposed RJPQ scheme with different

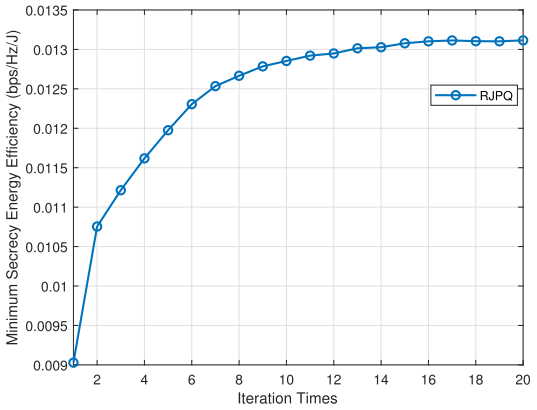

FIGURE 2. Convergence performance of the proposed algorithm 2 with T=90s.

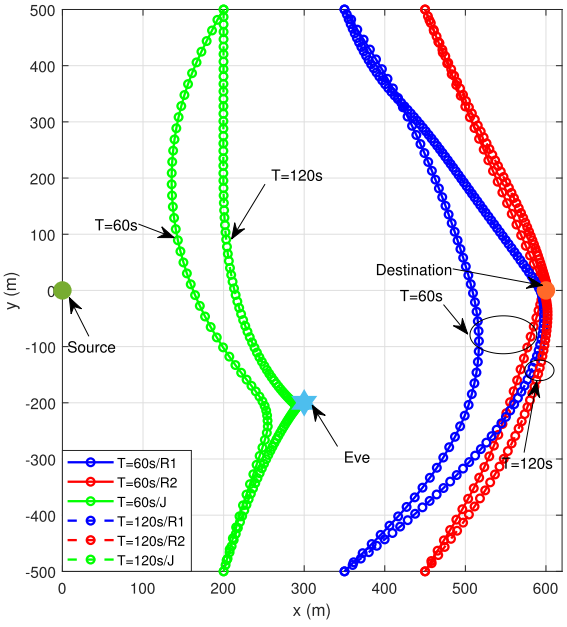

FIGURE 3. Trajectory comparison for the proposed algorithm with different periods T.

periods T. The S, D, and E nodes are marked by green dot, orange dot and blue hexagon, respectively. We adopt $T = 60s$ and $T = 120s$ in our simulations to represent insufficient and sufficient mission time, respectively. It can be drawn that the minimum flight period is T=50s, where all UAVs fly in similar trajectories from their initial points to the final points straightly. It can be observed that the RUAVs move closer to receivers while the JUAV fly closer to the eavesdropper in different time mission cases. When $T = 60s$, all RUAVs fly towards their receivers in arc path and then return to the final positions in the mission time. Meanwhile, the JUAV keeps away from the RUAV1 to reduce the interference and flies to a point near to the eavesdropper. When $T = 120s$, the RUAVs and JUAV have more sufficient time to get closer to receivers and eavesdropper. It is worth noting that the JUAV flies close to the eavesdropper straightly to save propulsion energy when $T = 120s$, which is significantly different from the behavior in the case of $T = 60s$. Comparing the two cases with different periods, we can find that the larger period T is enabled, the more degrees of freedom for UAV trajectory optimization can be available, and thus the better system performance can be achieved.

Fig.4 demonstrates the trajectories of UAV swarm obtained by RJPQ, RPQ, RJQ and RPQ-NJ schemes with the UAV flight duration $T = 90s$. It can be observed that the trajectories of RUAV2 obtained by the four schemes are similar. Specifically, the RUAV2 flies to the final location in an arc path and thus get close to the destination for better LOS link quality. It can also be observed that the trajectories of RUAV1 in the RPQ and RJQ schemes are similar to our proposed RJPQ scheme with longer flight distance. However, RUAV1 flies along a small arc path to be closer to source user in RPQ-NJ scheme. For the trajectory of JUAV, the simulation result in RJQ scheme without power optimization has a distinct difference from the proposed RJPQ scheme. The JUAV flies away from RUAVs and the destination over all time slots to reduce the interference for legitimate link. Therefore, the proposed RJPQ scheme improves the effectiveness of a friendly jammer while mitigating the interference to legitimate links with the shortest flight trajectory, which leads to a significant enhancement on system secrecy energy efficiency performance.

Fig.5 and Fig.6 present the MSEE and MASR performance versus UAV mission time T in different schemes, respectively. From these simulation results, we can see that the proposed RJPQ scheme achieves better performance by joint trajectory and transmit power optimization compared with RPQ and RJQ schemes, and therefore is a more effective method for system performance improvement. It is worth noting that the scheme without JUAV (RPQ-NJ) achieves an excellent SEE performance preceded only by RJPQ scheme, but the worst secrecy rate performance. The result reveals that introducing cooperative jammer UAV can greatly improve the system secrecy performance, although it will bring additional energy consumption. Besides, the MASR of all schemes grows up with the increasing of period T, while the MSEE has less

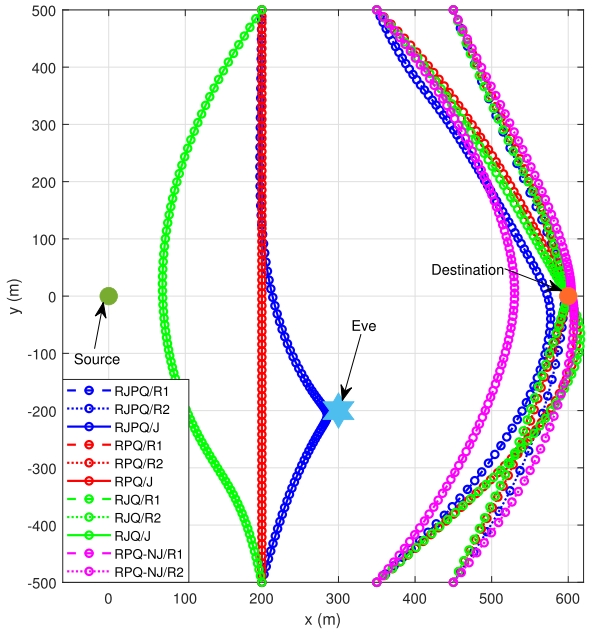

FIGURE 4. Trajectory comparison of the UAV swarm in three different schemes under T=90s.

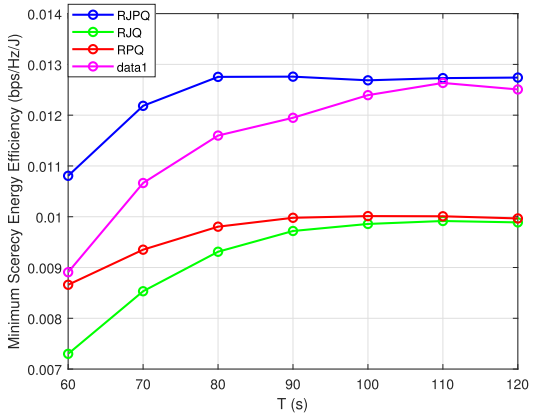

FIGURE 5. The minimum secrecy energy efficiency comparison in different schemes.

improvement after T increases to a certain value, due to the increasing of UAV propulsion energy consumption. Therefore, it is useless to increase the period T blindly for the MSEE improvement, and we can find an optimal mission time for UAV swarm in the practical scenarios with the consideration on MSEE maximization.

In Fig.7, we can get the details of UAV swarm flight in different schemes by observing the speed of all UAVs at each time slot. We divide each UAV trajectory into three stages: 1) flying to their quasi-stationary areas at high speed; 2) flying near to the E node or corresponding receivers at low speed; 3) flying to their final locations at high speed. Specifically, the JUAV's flight speed in RJPQ varies on a larger scale compared with that in RJQ because of effective power control. Since the receiver of RUAV1 is mobile, RUAV1 keeps a relatively stable medium speed in all schemes. Besides,

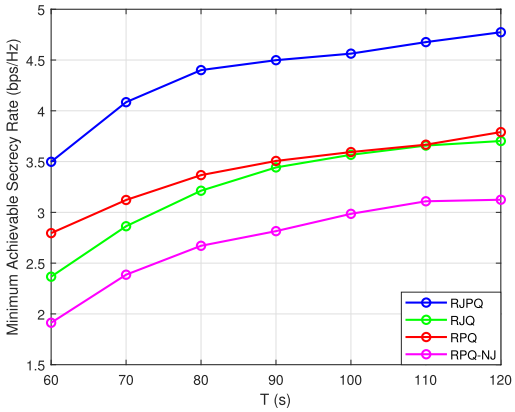

FIGURE 6. The minimum achievable secrecy rate comparison in different schemes.

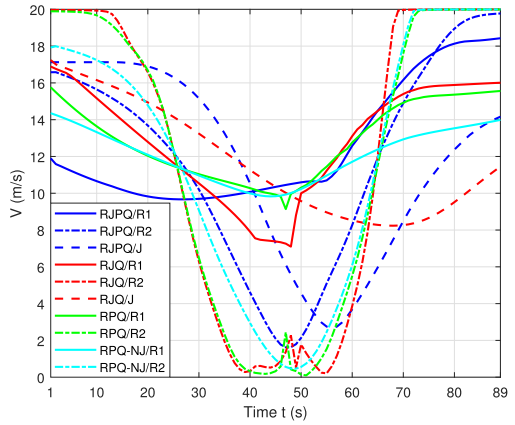

FIGURE 7. Speed of the UAV swarm at each slot in RJPQ scheme under T=90s.

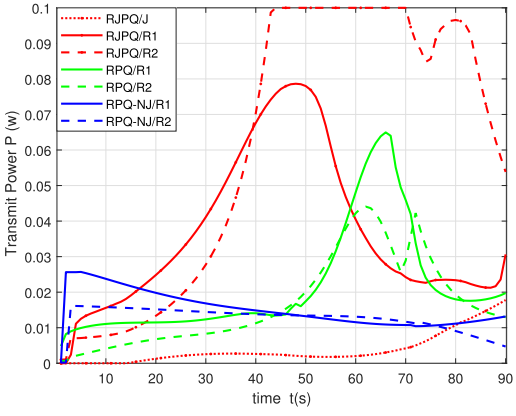

FIGURE 8. Transmit power of the UAV swarm at each slot under T=90s.

we can observe that the RUAV2 speed in all schemes varies in an area from zero to maximum speed, because RUAV2 tends to prolong the time flying near the destination to get better channel gain.

The transmit power of UAV swarm versus time is plotted in Fig.8. For RJPQ scheme, it can be observed that, at any time instant, the power of JUAV is lower than that

of RUAV to avoid excessive interference on legitimate links. Besides, when RUAVs are getting closer to their corresponding legitimate receivers, they tend to increase transmit power to improve achievable rates. In the RPQ scheme, all the RUAVs transmit information with lower power, due to the fixed track of JUAV. However, for RPQ-NJ scheme, the RUAV transmit power maintains a small value to avoid wiretapping. Without power control, communication interference is merely mitigated by optimizing the trajectory of UAV swarm. Consequently, a joint power control and trajectory design can provide more degrees of freedom to mitigate legitimate link interference and thus achieves higher SEE performance.

V. CONCLUSION

This article has studied the secrecy and energy efficiency issue in a UAV swarm assisted multi-hop mobile relay system. A novel cooperative scheme with RUAV and JUAV has been proposed to improve the system secrecy performance. By exploiting the UAV's high mobility, we have maximized the secrecy energy efficiency by jointly optimizing the trajectory and transmit power of RUAV and JUAV, subject to the constraints of UAV mobility, maximum transmit power and information-causality. By means of the successive convex optimization techniques, Dinkelbach method and block coordinate descent method, an efficient iterative algorithm has been proposed to solve the formulated non-convex fractional optimization problem, which is guaranteed to converge. Extensive simulations and numerical results demonstrate that compared with the benchmark schemes, the proposed joint optimization scheme can achieve significant improvement on secrecy rate and energy efficiency. Moreover, the novel cooperative UAV swarm scheme can be further extended by considering the different channel models, unknown nodes' locations, real-time communications, etc., which will be left as future work.

REFERENCES

[1] Y. Zeng, R. Zhang, and T. J. Lim, "Wireless communications with unmanned aerial vehicles: Opportunities and challenges," *IEEE Commun. Mag.*, vol. 54, no. 5, pp. 36–42, May 2016, doi: 10.1109/MCOM.2016.7470933.

[2] B. Alzahrani, O. S. Oubbati, A. Barnawi, M. Atiquzzaman, and D. Alghazzawi, "UAV assistance paradigm: State-of-the-art in applications and challenges," *J. Netw. Comput. Appl.*, vol. 166, Sep. 2020, Art. no. 102706, doi: 10.1016/j.jnca.2020.102706.

[3] O. S. Oubbati, M. Atiquzzaman, T. A. Ahanger, and A. Ibrahim, "Softwarization of UAV networks: A survey of applications and future trends," *IEEE Access*, vol. 8, pp. 98073–98125, 2020, doi: 10.1109/ACCESS.2020.2994494.

[4] J. Lyu, Y. Zeng, R. Zhang, and T. J. Lim, "Placement optimization of UAV-mounted mobile base stations," *IEEE Commun. Lett.*, vol. 21, no. 3, pp. 604–607, Mar. 2017, doi: 10.1109/LCOMM.2016.2633248.

[5] Q. Wu, Y. Zeng, and R. Zhang, "Joint trajectory and communication design for multi-UAV enabled wireless networks," *IEEE Trans. Wireless Commun.*, vol. 17, no. 3, pp. 2109–2121, Mar. 2018, doi: 10.1109/TWC.2017.2789293.

[6] Y. Zeng, R. Zhang, and T. J. Lim, "Throughput maximization for UAV-enabled mobile relaying systems," *IEEE Trans. Commun.*, vol. 64, no. 12, pp. 4983–4996, Dec. 2016, doi: 10.1109/TCOMM.2016.2611512.

[7] S. Zhang, H. Zhang, Q. He, K. Bian, and L. Song, "Joint trajectory and power optimization for UAV relay networks," *IEEE Commun. Lett.*, vol. 22, no. 1, pp. 161–164, Jan. 2018, doi: 10.1109/LCOMM.2017.2763135.

[8] G. Zhang, Q. Wu, M. Cui, and R. Zhang, "Securing UAV communications via joint trajectory and power control," *IEEE Trans. Wireless Commun.*, vol. 18, no. 2, pp. 1376–1389, Feb. 2019, doi: 10.1109/TWC.2019.2892461.

[9] X. Sun, W. Yang, and Y. Cai, "Secure communication in NOMA-assisted millimeter-wave SWIPT UAV networks," *IEEE Internet Things J.*, vol. 7, no. 3, pp. 1884–1897, Mar. 2020, doi: 10.1109/JIOT.2019.2957021.

[10] M. Xu, Y. Chen, and W. Wang, "A two-stage game framework to secure transmission in two-tier UAV networks," *IEEE Trans. Veh. Technol.*, vol. 69, no. 11, pp. 13728–13740, Nov. 2020, doi: 10.1109/TVT.2020.3026184.

[11] X. Zhou, Q. Wu, S. Yan, F. Shu, and J. Li, "UAV-enabled secure communications: Joint trajectory and transmit power optimization," *IEEE Trans. Veh. Technol.*, vol. 68, no. 4, pp. 4069–4073, Apr. 2019, doi: 10.1109/TVT.2019.2900157.

[12] Y. Li, R. Zhang, J. Zhang, S. Gao, and L. Yang, "Cooperative jamming for secure UAV communications with partial eavesdropper information," *IEEE Access*, vol. 7, pp. 94593–94603, 2019, doi: 10.1109/ACCESS.2019.2926741.

[13] R. Li, Z. Wei, L. Yang, D. W. K. Ng, J. Yuan, and J. An, "Resource allocation for secure multi-UAV communication systems with multi-eavesdropper," *IEEE Trans. Commun.*, vol. 68, no. 7, pp. 4490–4506, Jul. 2020, doi: 10.1109/TCOMM.2020.2983040.

[14] J. Tang, G. Chen, and J. P. Coon, "Secrecy performance analysis of wireless communications in the presence of UAV jammer and randomly located UAV eavesdroppers," *IEEE Trans. Inf. Forensics Security*, vol. 14, no. 11, pp. 3026–3041, Nov. 2019, doi: 10.1109/TIFS.2019.2912074.

[15] R. Ma, W. Yang, Y. Zhang, J. Liu, and H. Shi, "Secure mmWave communication using UAV-enabled relay and cooperative jammer," *IEEE Access*, vol. 7, pp. 119729–119741, 2019, doi: 10.1109/ACCESS.2019.2933231.

[16] Y. Zhang, Z. Mou, F. Gao, J. Jiang, R. Ding, and Z. Han, "UAV-enabled secure communications by multi-agent deep reinforcement learning," *IEEE Trans. Veh. Technol.*, vol. 69, no. 10, pp. 11599–11611, Oct. 2020, doi: 10.1109/TVT.2020.3014788.

[17] Y. Zeng and R. Zhang, "Energy-efficient UAV communication with trajectory optimization," *IEEE Trans. Wireless Commun.*, vol. 16, no. 6, pp. 3747–3760, Jun. 2017, doi: 10.1109/TWC.2017.2688328.

[18] Y. Zeng, J. Xu, and R. Zhang, "Energy minimization for wireless communication with rotary-wing UAV," *IEEE Trans. Wireless Commun.*, vol. 18, no. 4, pp. 2329–2345, Apr. 2019, doi: 10.1109/TWC.2019.2902559.

[19] M. Hua, Y. Wang, Q. Wu, H. Dai, Y. Huang, and L. Yang, "Energy-efficient cooperative secure transmission in multi-UAV-enabled wireless networks," *IEEE Trans. Veh. Technol.*, vol. 68, no. 8, pp. 7761–7775, Aug. 2019, doi: 10.1109/TVT.2019.2924180.

[20] J. Miao and Z. Zheng, "Cooperative jamming for secure UAV-enabled mobile relay system," *IEEE Access*, vol. 8, pp. 48943–48957, 2020, doi: 10.1109/ACCESS.2020.2980242.

[21] J. Fan, M. Cui, G. Zhang, and Y. Chen, "Throughput improvement for multi-hop UAV relaying," *IEEE Access*, vol. 7, pp. 147732–147742, 2019, doi: 10.1109/ACCESS.2019.2946353.

[22] Y. Chen, N. Zhao, Z. Ding, and M.-S. Alouini, "Multiple UAVs as relays: Multi-hop single link versus multiple dual-hop links," *IEEE Trans. Wireless Commun.*, vol. 17, no. 9, pp. 6348–6359, Sep. 2018, doi: 10.1109/TWC.2018.2859394.

[23] A. Mukherjee and A. L. Swindlehurst, "Detecting passive eavesdroppers in the MIMO wiretap channel," in *Proc. IEEE Int. Conf. Acoust., Speech Signal Process. (ICASSP)*, Kyoto, Japan, Mar. 2012, pp. 2809–2812, doi: 10.1109/ICASSP.2012.6288501.

[24] M. Mozaffari, W. Saad, M. Bennis, and M. Debbah, "Mobile unmanned aerial vehicles (UAVs) for energy-efficient Internet of Things communications," *IEEE Trans. Wireless Commun.*, vol. 16, no. 11, pp. 7574–7589, Nov. 2017, doi: 10.1109/TWC.2017.2751045.

[25] X. Zhang, J. Zhang, J. Xiong, L. Zhou, and J. Wei, "Energy-efficient multi-UAV-enabled multiaccess edge computing incorporating NOMA," *IEEE Internet Things J.*, vol. 7, no. 6, pp. 5613–5627, Jun. 2020, doi: 10.1109/JIOT.2020.2980035.

[26] *LTE Unmanned Aircraft Systems*, Qualcomm Technol., San Diego, CA, USA, Trial Rep. V.1.0.1, 2017.

[27] D. W. Matolak and R. Sun, "Air–ground channel characterization for unmanned aircraft systems—Part III: The suburban and near-urban environments," *IEEE Trans. Veh. Technol.*, vol. 66, no. 8, pp. 6607–6618, Aug. 2017, doi: 10.1109/TVT.2017.2659651.

[28] S. Boyd and L. Vandenberghe, *Convex Optimization*. Cambridge, U.K.: Cambridge Univ. Press, 2004.

[29] A. T. Phillips, *Quadratic Fractional Programming: Dinkelbach Method* (Encyclopedia of Optimization), C. Floudas and P. Pardalos, Eds. Boston, MA, USA: Springer, 2008. [Online]. Available: https://doi.org/10.1007/978-0-387-74759-0535

[30] K. T. K. Cheung, S. Yang, and L. Hanzo, "Achieving maximum energy-efficiency in multi-relay OFDMA cellular networks: A fractional programming approach," *IEEE Trans. Commun.*, vol. 61, no. 8, pp. 2746–2757, Jul. 2013, doi: 10.1109/TCOMM.2013.13.120727.

[31] M. Grant and S. Boyd. (2016). *CVX: MATLAB Software for Disciplined Convex Programming*. [Online]. Available: http://cvxr.com/cvx

[32] D. P. Bertsekas, *Nonlinear Programming*. Belmont, MA, USA: Athena Scientific, 1999.

JIANSONG MIAO received the B.Eng. degree in communication engineering from Jilin University in 2001 and the Ph.D. degree in communication and information system from the Beijing University of Posts and Telecommunications. He has participated in a number of national, provincial and ministerial and cooperative scientific research projects as a main researcher. He has authored or coauthored over 20 articles. His current research interests include broadband wireless access networks, unmanned aerial vehicle-assisted communication systems, and mobile ad hoc networks.

HAIRUI LI was born in Heilongjiang, China, in 1997. She received the B.Eng. degree in communication engineering from the China University of petroleum in 2019. She is currently pursuing the master's degree with the Beijing university of Posts and Telecommunications. Her current research interests include unmanned aerial vehicle (UAV) communications, transceiver optimization for wireless systems, energy efficiency, UAV-assisted communication systems, and UAV-assisted MEC systems.

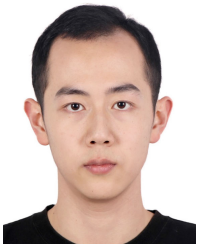

ZIYUAN ZHENG was born in Beijing, China, in 1996. He received the B.Eng. degree in communication engineering from the Beijing University of Posts and Telecommunications, in 2018, where he is currently pursuing the master's degree. His current research interests include unmanned aerial vehicle (UAV) communications, transceiver optimization for wireless systems, physical layer security, and UAV-assisted communication systems.

CHU WANG was born in Nei Monggol, China, in 1997. He received the B.Eng. degree in communication engineering from the Harbin Institute of Technology, in 2019. He is currently pursuing the master's degree with the Beijing University of Posts and Telecommunications. His current research interests include unmanned aerial vehicle communications and transceiver optimization for wireless systems.